



KNO

Krajowy Naukowy
Ośrodek Wiedzący



NATIONAL SCIENCE CENTRE
POLAND

Kinetic modeling of collisionless shocks: selected recent results relevant to high- energy astrophysical sources

Jacek Niemiec

Institute of Nuclear Physics, Polish Academy of Sciences, Kraków, Poland

Collaborators:

[Artem Bohdan](#), Desy-Zeuthen, Germany

[Oleh Kobzar](#) - Cracow Institute of Technology, Kraków, Poland

[Takanobu Amano](#), [Masahiro Hoshino](#) - University of Tokyo, Japan

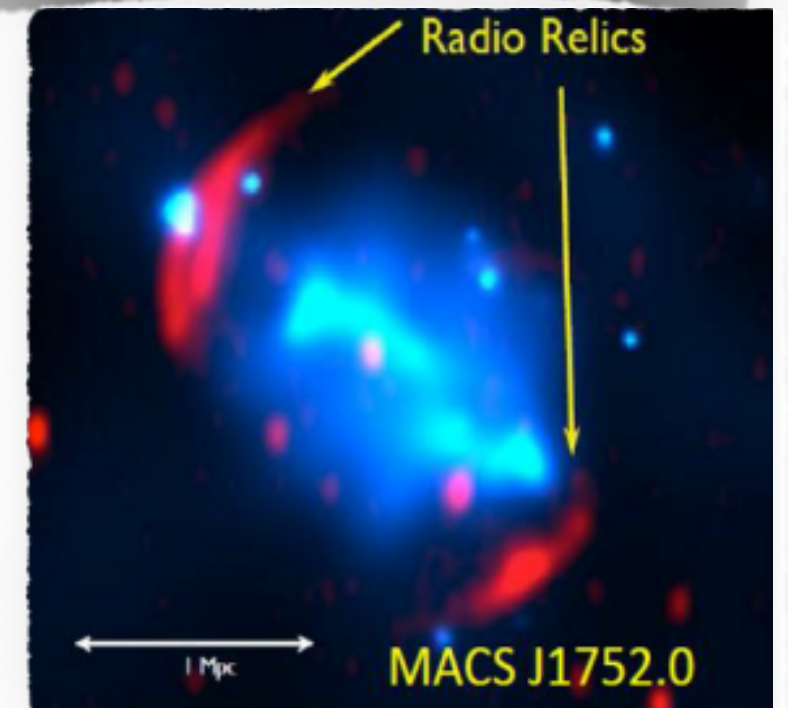
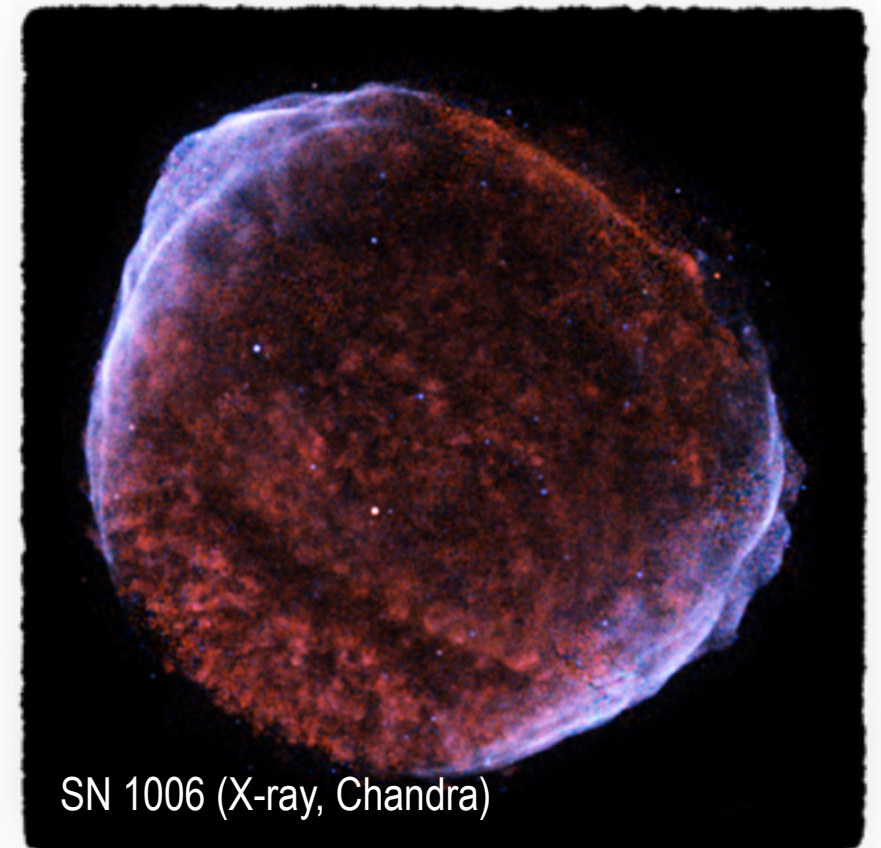
[Yosuke Matsumoto](#) - Chiba University, Japan

[Shuichi Matsukiyo](#) - Kyushu University, Japan

[Martin Pohl](#) - Desy-Zeuthen/University of Potsdam, Germany

Collisionless shocks in space

- Cosmic shocks are in most cases collisionless
- structure and particle acceleration at such shocks involve complex kinetic plasma processes, well beyond MHD description
- radiation emission is governed by the efficiency of CR acceleration, that is determined by the injection processes



Alfvenic Mach number: $M_A = \frac{v_{sh}}{v_A}$

Sonic Mach number: $M_s = \frac{v_{sh}}{c_s}$

Plasma beta: $\beta = p_{th}/p_{mag}$

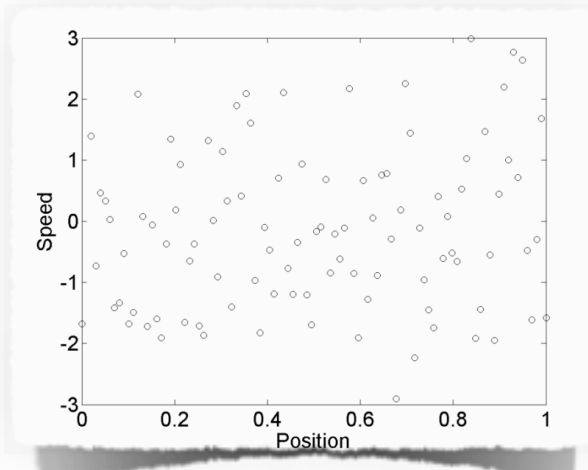
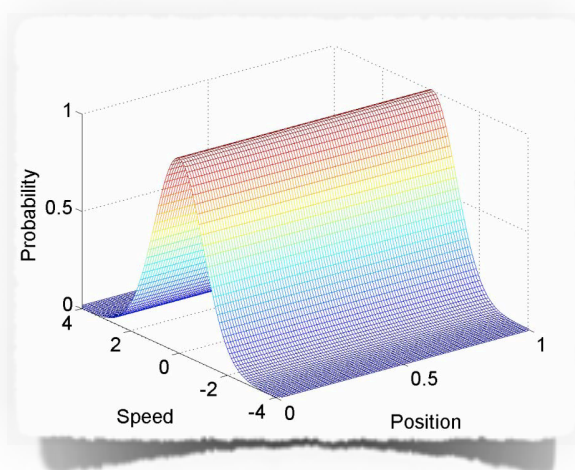
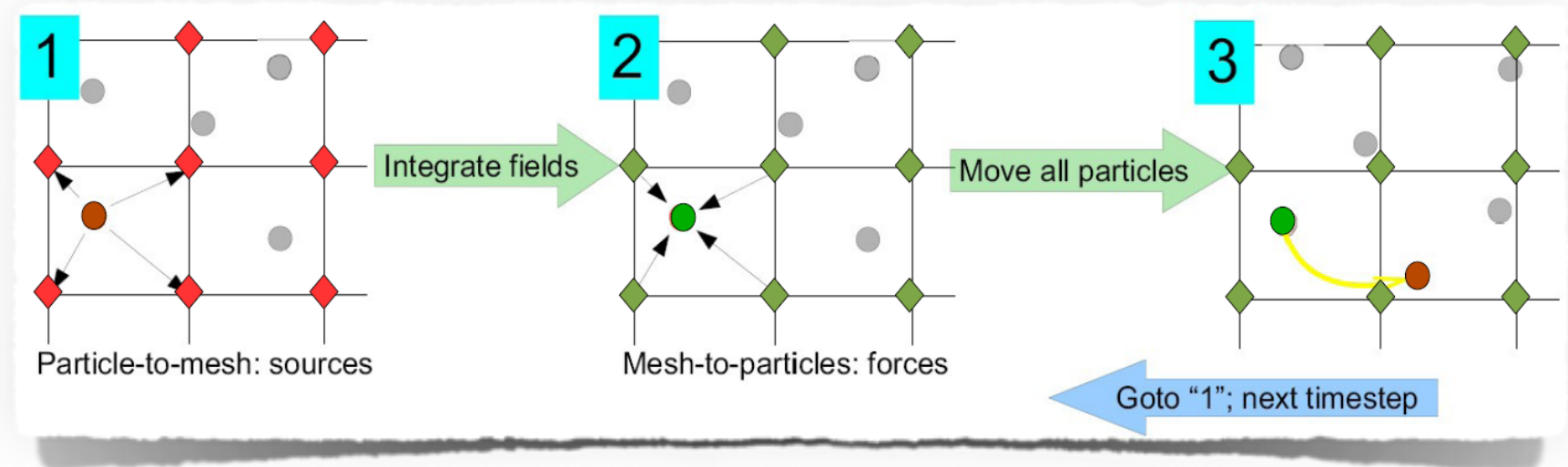
$$v_A = \frac{B_0}{\sqrt{\mu_0(N_e m_e + N_i m_i)}}$$

$$c_s = \sqrt{2\Gamma k_B T_i / m_i}$$

White – optical (Hubble)
 Blue – X-ray (Chandra)
 Red – radio (VLA)

Method of Particle-In-Cell Simulations

- Fully self-consistent description of collisionless plasma:
 - Vlasov equation (kinetic theory; **time evolution of particle distribution function** $f(\mathbf{x}, \mathbf{v}, t)$ in phase-space) + Maxwell's equations
- **Particle-In-Cell** modeling - an *ab-initio* method of Vlasov equation solution through:
 - integration of Maxwell's equations on a numerical grid
 - integration of relativistic particle equations of motion in collective self-consistent EM field

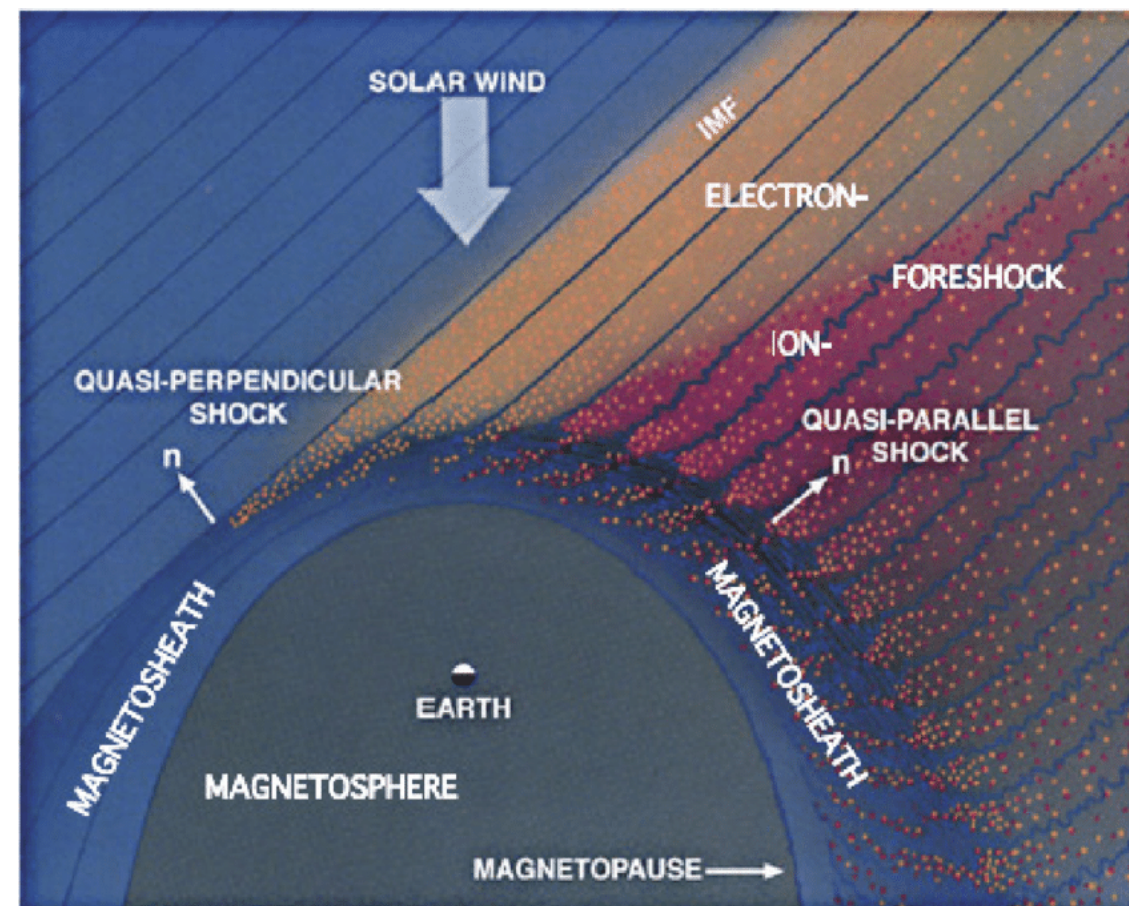


Particle distribution function represented by **macro**particles on a numerical grid.
(Macroparticles represent a small volume of particle phase-space; equations of motion as for realistic particles)

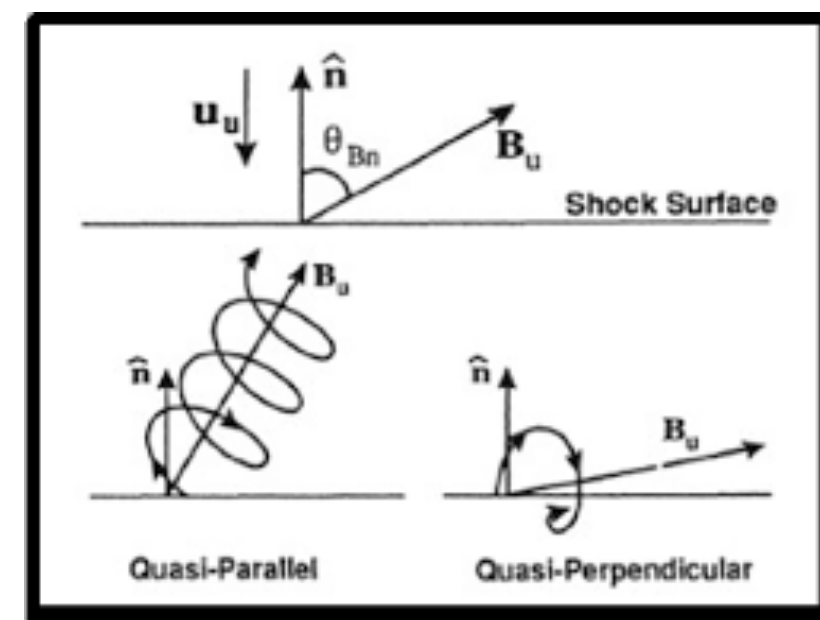
Particle acceleration at nonrelativistic shocks

$$v_{\text{sh}}/c \ll 1$$

- Particle acceleration at collisionless shocks depends on plasma parameters (sonic and Alfvénic Mach number, plasma beta, shock speed, shock obliquity,...)
- Most studies up to now concern low beta ($\beta < 1$) shocks (Earth's bow shock, interplanetary shocks, SNR shocks)
- Emerging picture:
 - supercritical shocks - reflected ions drive plasma instabilities upstream
 - efficient **proton** acceleration at **quasi-parallel** (Q_{\parallel}) shocks
 - efficient **electron** acceleration at **quasi-perpendicular** (Q_{\perp}) shocks



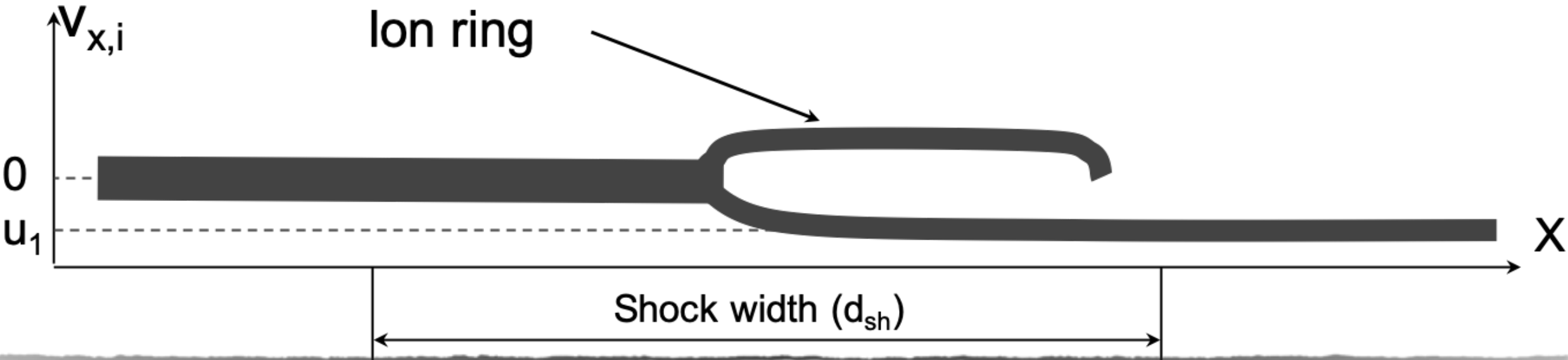
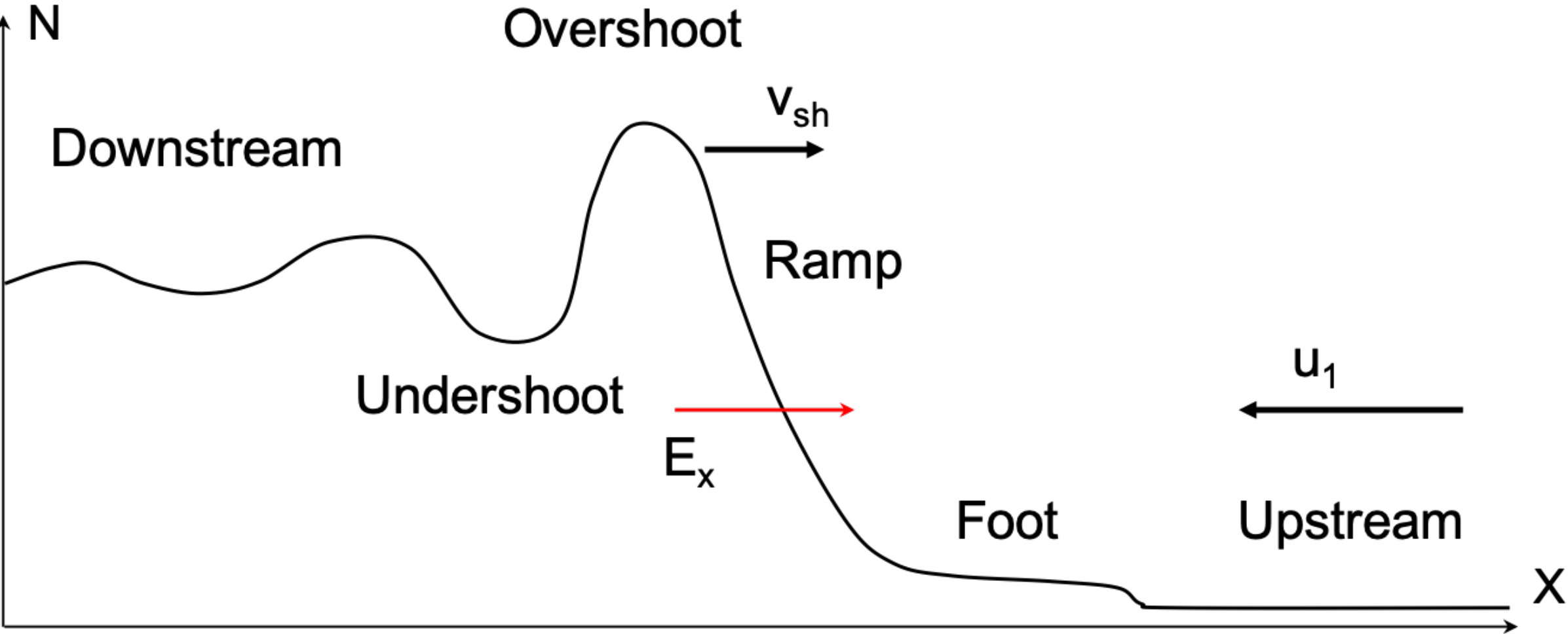
Shock obliquity



Selected topics:

- Magnetic field amplification at high Mach number shocks (SNRs, planetary bow shocks) $M_s > 10$, $M_A > 10$, $\beta \sim 1$
- Electron heating in high Mach number shocks
- Short review of proton and electron acceleration in **low Mach number** shocks propagating in high-beta plasmas (galaxy cluster shocks): $M_s < 5$, $M_A < 10$, $\beta \gg 1$
- Electron injection in low M_s shocks with multi-scale turbulence

Microstructure of a quasi-perpendicular high Mach number shock



Microstructure of a quasi-perpendicular high Mach number shock

Downstream

Overshoot

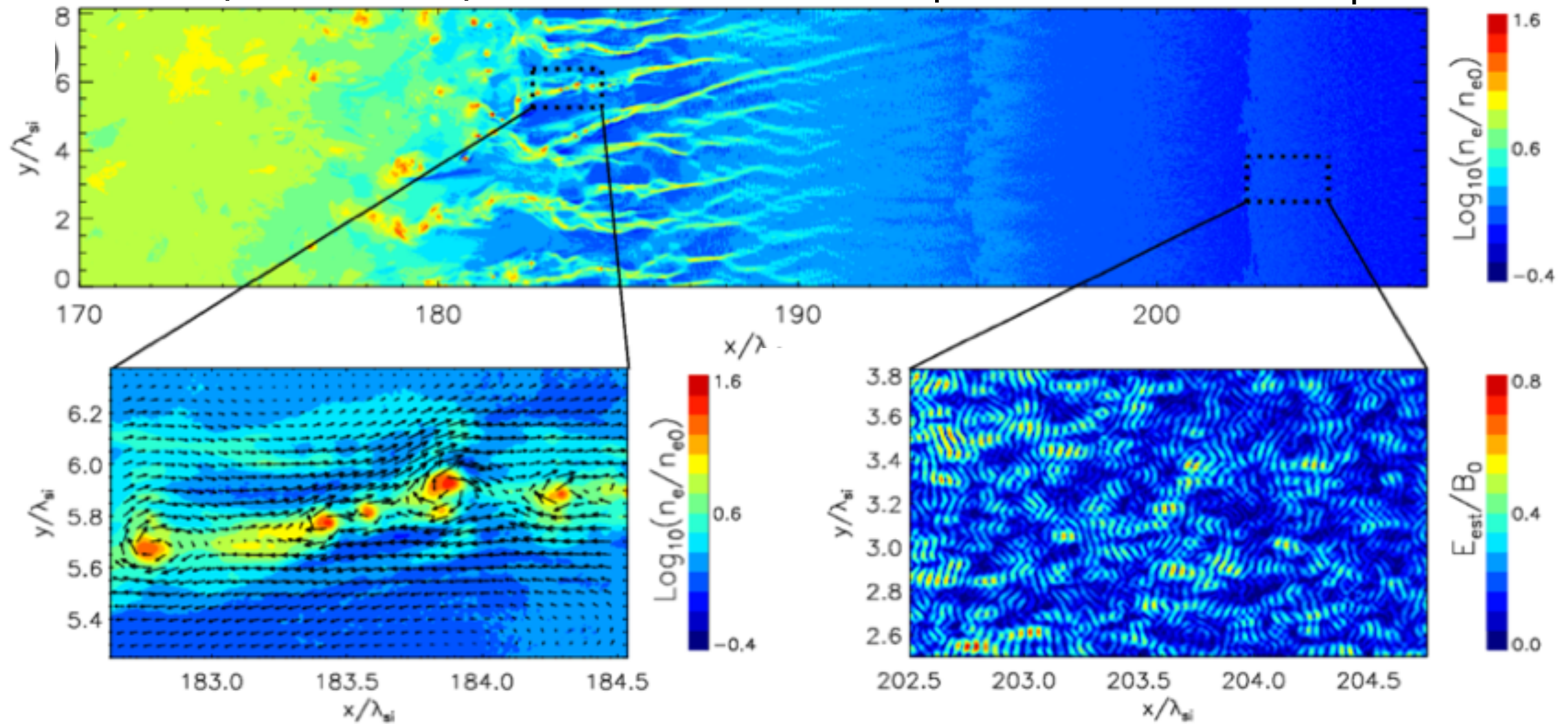
Ramp

Foot

Upstream

Weibel instability
Magnetic reconnection

Buneman instability
(shock surfing acc.)



Simulation parameters

$$M_A = 23 - 150$$

$$\beta_e = 0.0005, 0.5$$

$$V_0 = 0.2c$$

$$m_i/m_e = 50 - 400$$

Saturn's bow shock

$$M_A \approx 5 - 200$$

$$\beta_e \approx 0.01 - 1$$

$$V_0 \approx 500 \text{ km/s} \approx 0.0017c$$

$$m_i/m_e = 1836$$

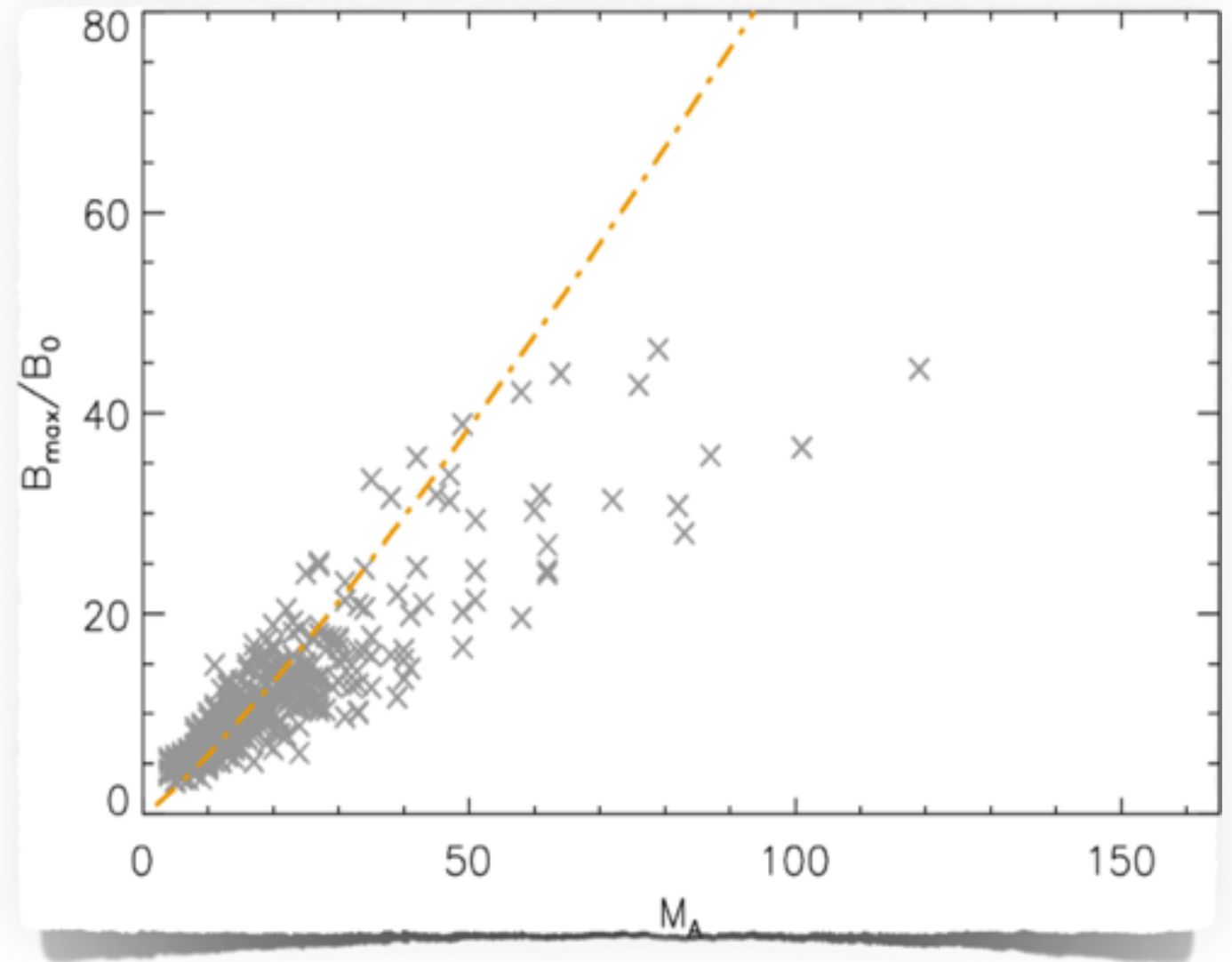
Runs	m_i/m_e	M_A	M_s	
			*1	*2
A1, A2	50	22.6	1104	35
B1, B2	100	31.8	1550	49
C1, C2	100	46	2242	71
D1, D2	200	32	1550	49
E1, E2	200	44.9	2191	69
F1, F2	400	68.7	3353	106
G1 [†] , G2	50	100	4870	154
H1 [†] , H2	50	150	7336	232

Magnetic field amplification

Bohdan et al., Phys. Rev. Lett. 126, 095101 (2021)

Saturn's bow shock: [in-situ](#) measurements of magnetic field

- strong correlation between B_{\max}/B_0 and M_A
- [Leroy's model](#) (Leroy 1983) - based on plasma compression only. Multi-dimensional effects not accounted for
- PIC simulations, in-situ measurements (Sundberg 2017) and laboratory experiments (Fiuza 2020) suggest that high- M_A shocks are [Weibel-instability mediated](#)

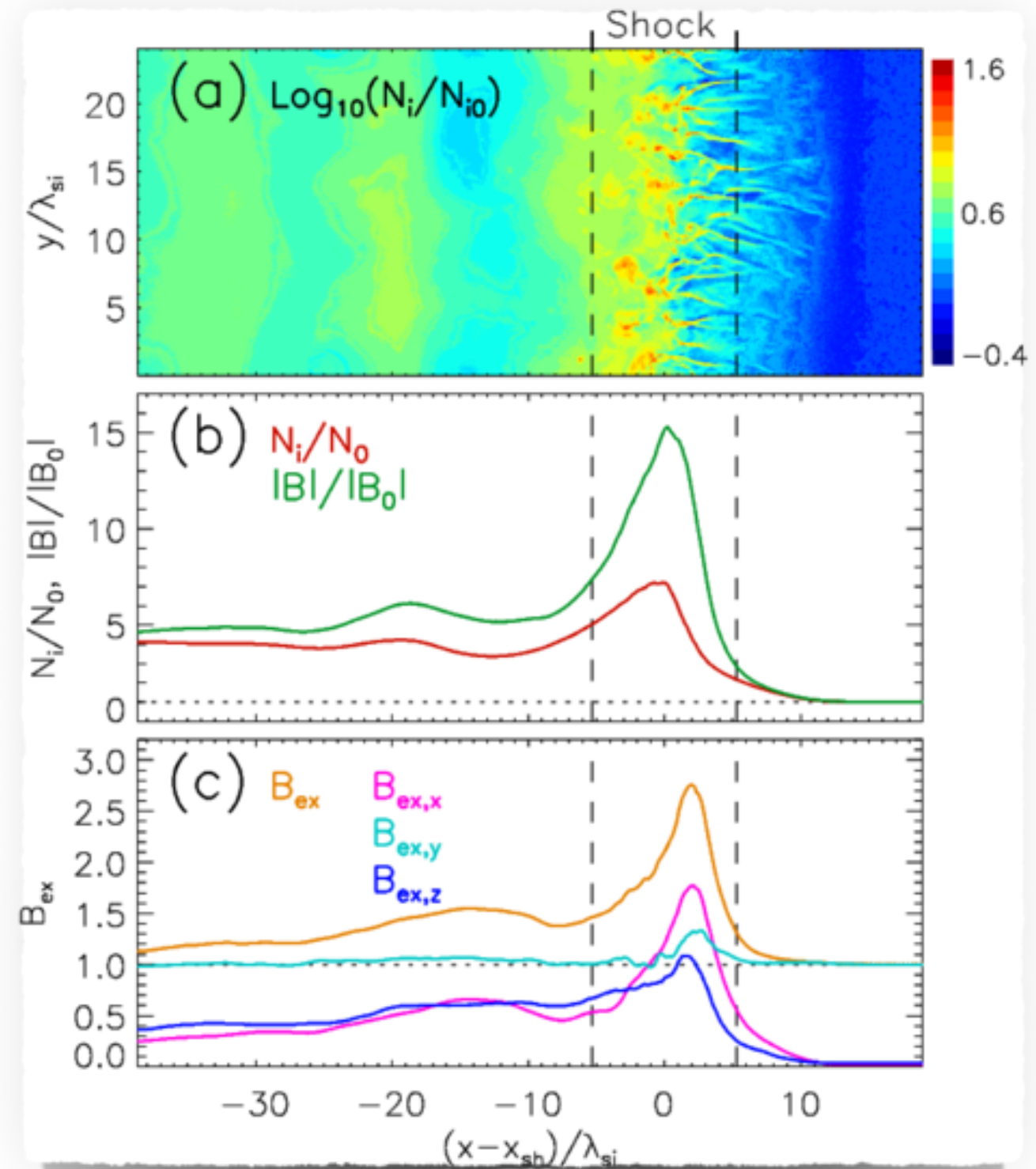


Density and magnetic field profiles ($M_A=32$)

- density compression does not follow Leroy's model
- extra magnetic field:

$$B_{\text{ex},l} = \frac{|B_l|}{|B_0|} \frac{|N_0|}{|N_i|}, \quad l = x, y, z$$

- If $B_{\text{ex}}=1$, then magnetic field amplified due to plasma compression only
- B_x and B_z components amplified due to the Weibel instability



Magnetic field strength and energy

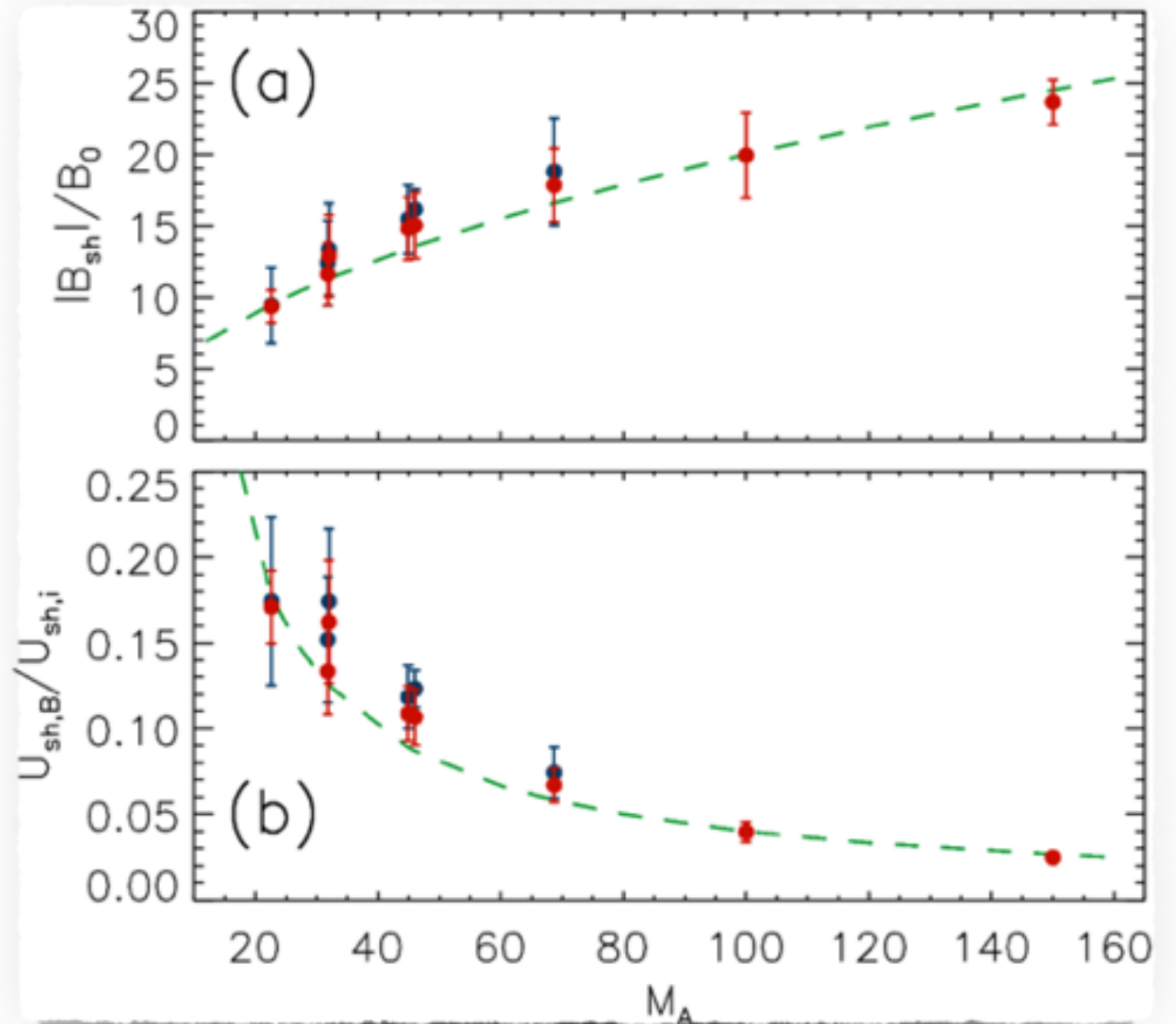
The magnetic field strength:

$$|B_{\text{sh}}| \approx 2\sqrt{M_A} B_0$$

The magnetic field energy:

$$\frac{U_{\text{sh,B}}}{U_{\text{sh,i}}} \approx \frac{4}{M_A}$$

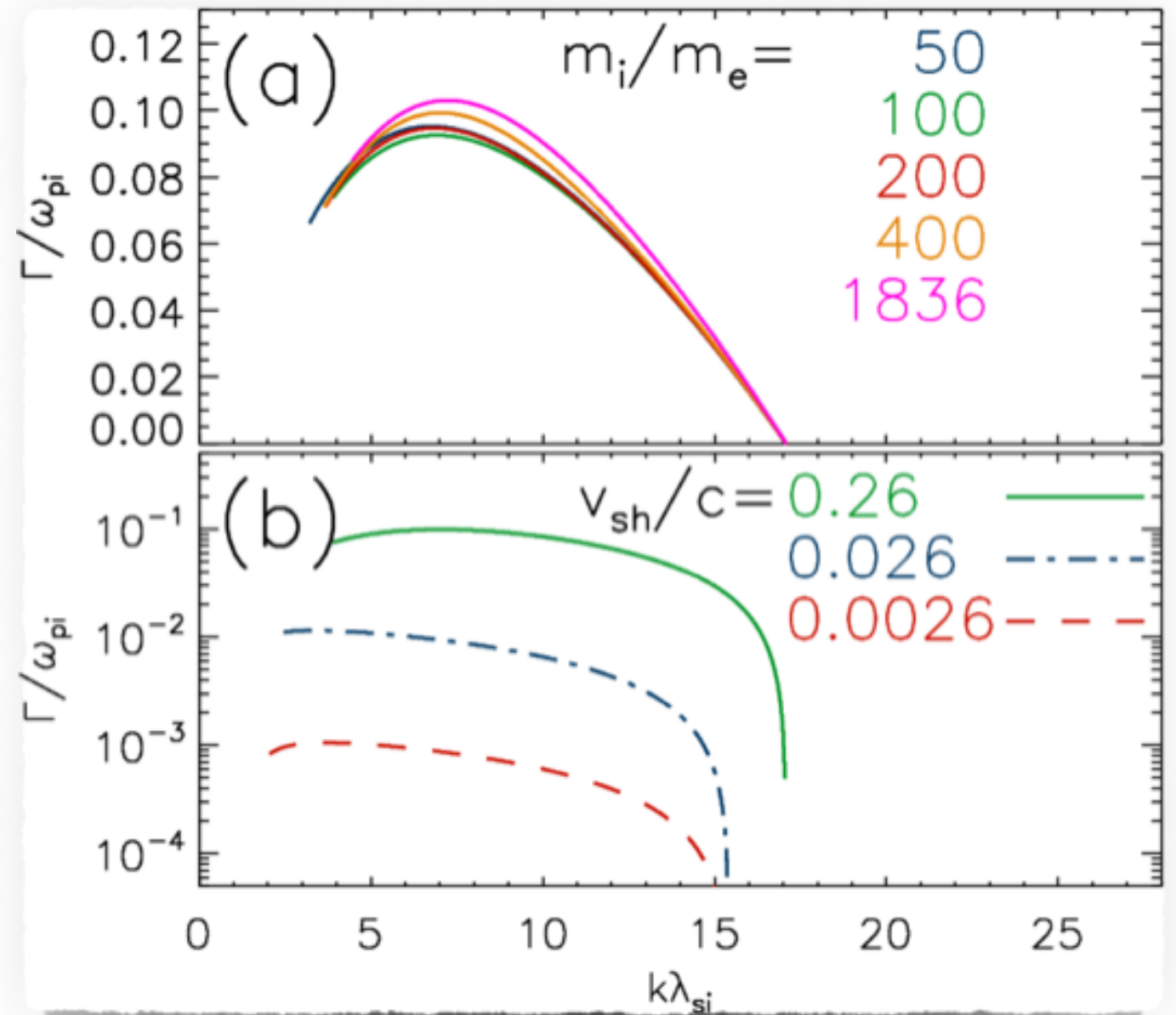
Does not depend on mass ratio and the upstream plasma beta.



The Weibel instability growth rate

- linear analysis for the parameters at the shock ramp
- growth rate of the most unstable Weibel mode

$$\frac{\Gamma_{\max}}{\omega_{pi}} \propto v_{sh} \quad \text{or} \quad \frac{\Gamma_{\max}}{\Omega_i} \propto M_A$$



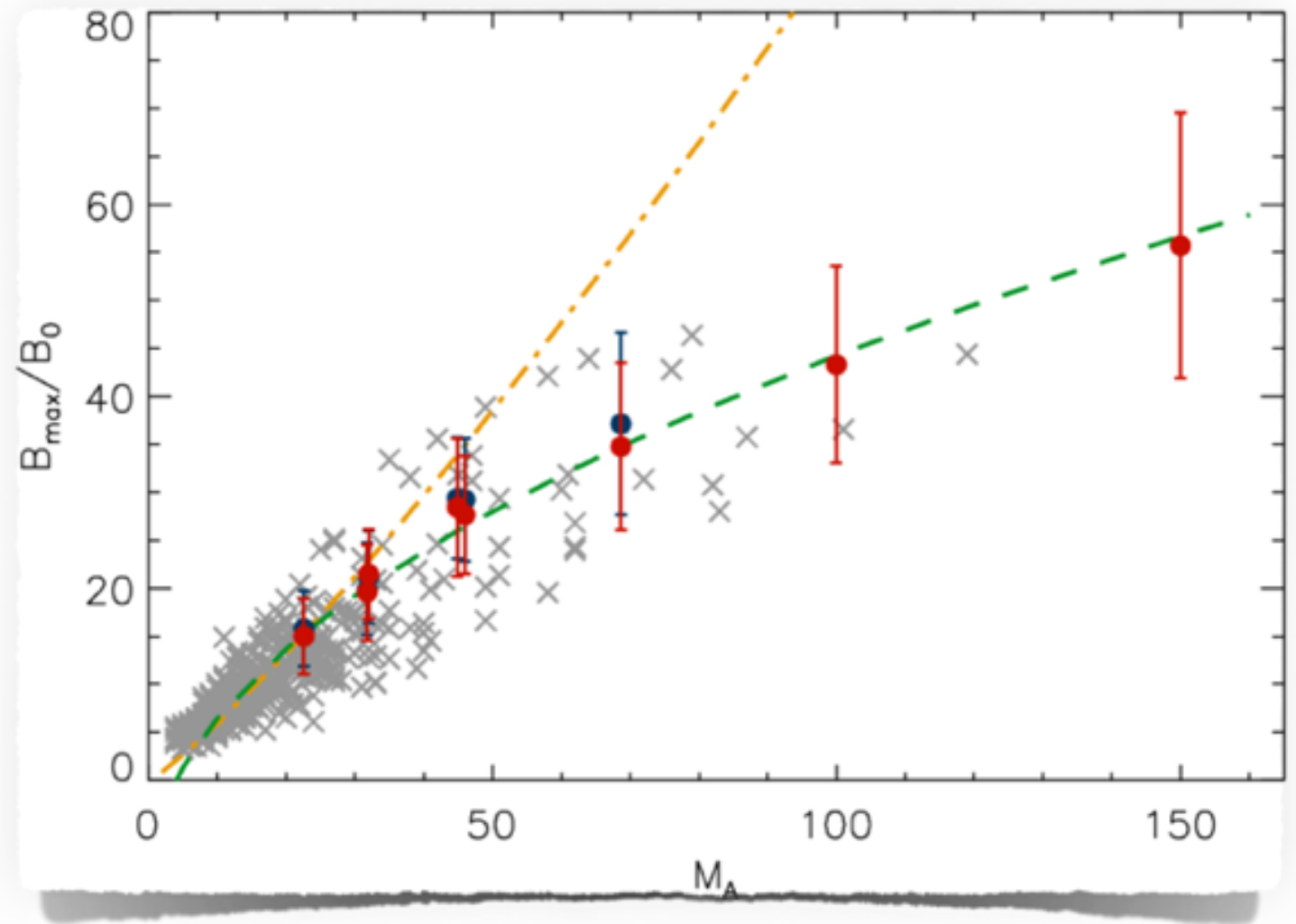
Magnetic field amplification: in-situ vs. PIC

- × In-situ measurements
- PIC simulation data
- Leroy's model

$$B_{\text{over}} \approx 0.4 B_0 M_A^{7/6}$$

- New model

$$\frac{B_{\text{max}}}{B_0} = 5.5 \left(\sqrt{M_A} - 2 \right)$$



Electron heating

Bohdan et al., ApJ 904, 12 (2020)

Electron heating in high Mach number shocks

A part of the upstream kinetic energy is converted to the thermal particle energy. Rankine-Hugoniot relations read ($\Gamma_p=5/3$):

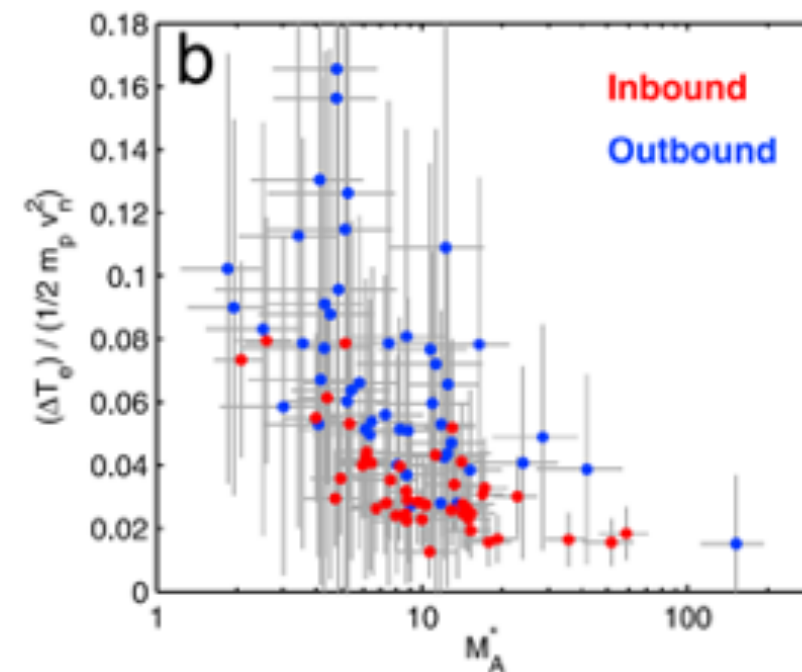
$$\rho_1/\rho_2 \approx 4$$

$$T_2/T_1 = 5/16 M_s^2$$

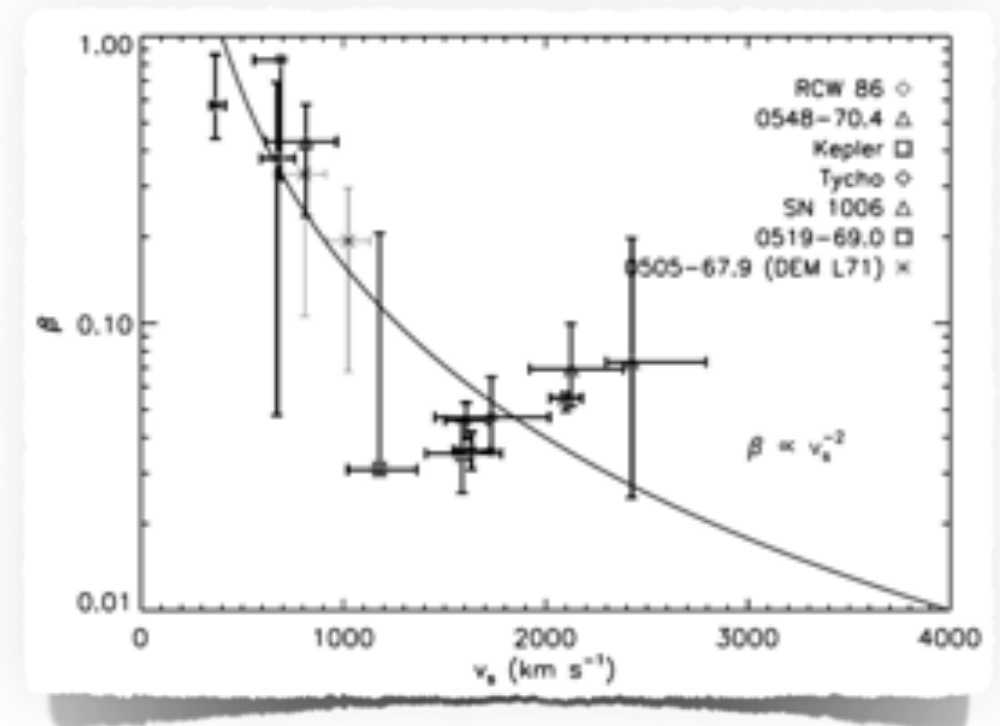
If there is no energy exchange between ions and electrons then

$$T_{2,e}/T_{2,i} = m_e/m_i$$

Observed temperature ratio: $T_{2,e}/T_{2,i} \approx 0.03 - 0.5$



Saturn's bow shock
(Masters 2011)



SNR shocks
(val Adelsberg 2008)

Electron heating model

The downstream electron energy $\varepsilon_e \approx (0.1-0.2) \cdot m_i v_{sh}^2$ and can be

expressed as
$$\varepsilon_e = \sum_a \varepsilon_a = \sum_a \alpha_a F_a m_i v_{sh}^2$$

Three stages of modeling:

1. Find all heating processes

Shock structure knowledge, individual and collective particle tracing analysis

2. Determine scaling properties: $F_a \equiv F_a(M_A, m_i/m_e, v_{sh})$

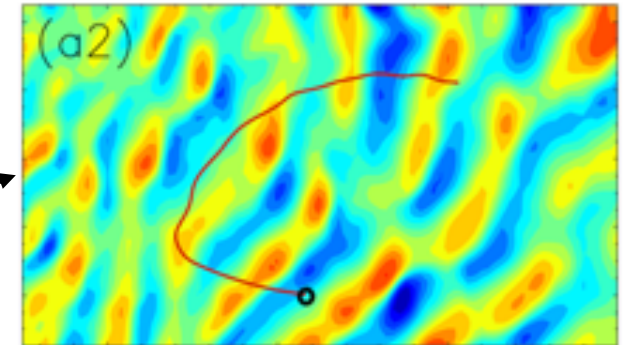
Physics of plasma instabilities, individual and collective particle tracing analysis

3. Calculation of efficiency coefficients using simulation data: α_a

Energy history of particle sets

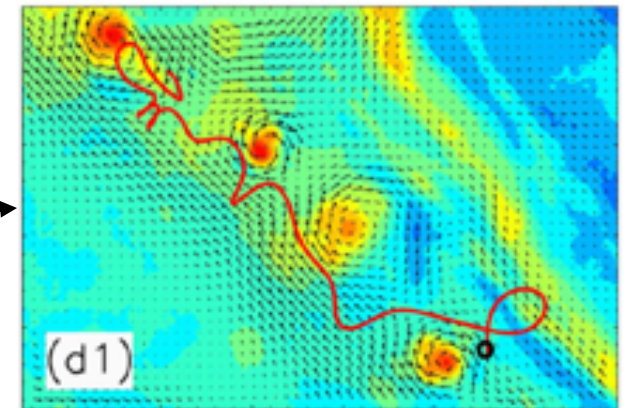
Electron heating processes

1. Shock-surfing acceleration (SSA) (Shimada 2001)



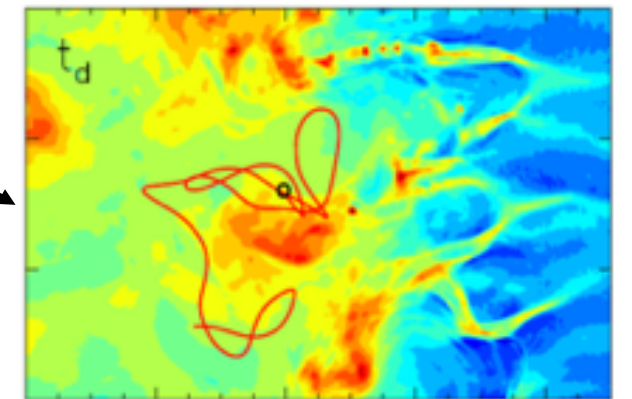
2. The shock potential (reflects ions, heats electrons)

3. Magnetic reconnection (Matsumoto 2015)



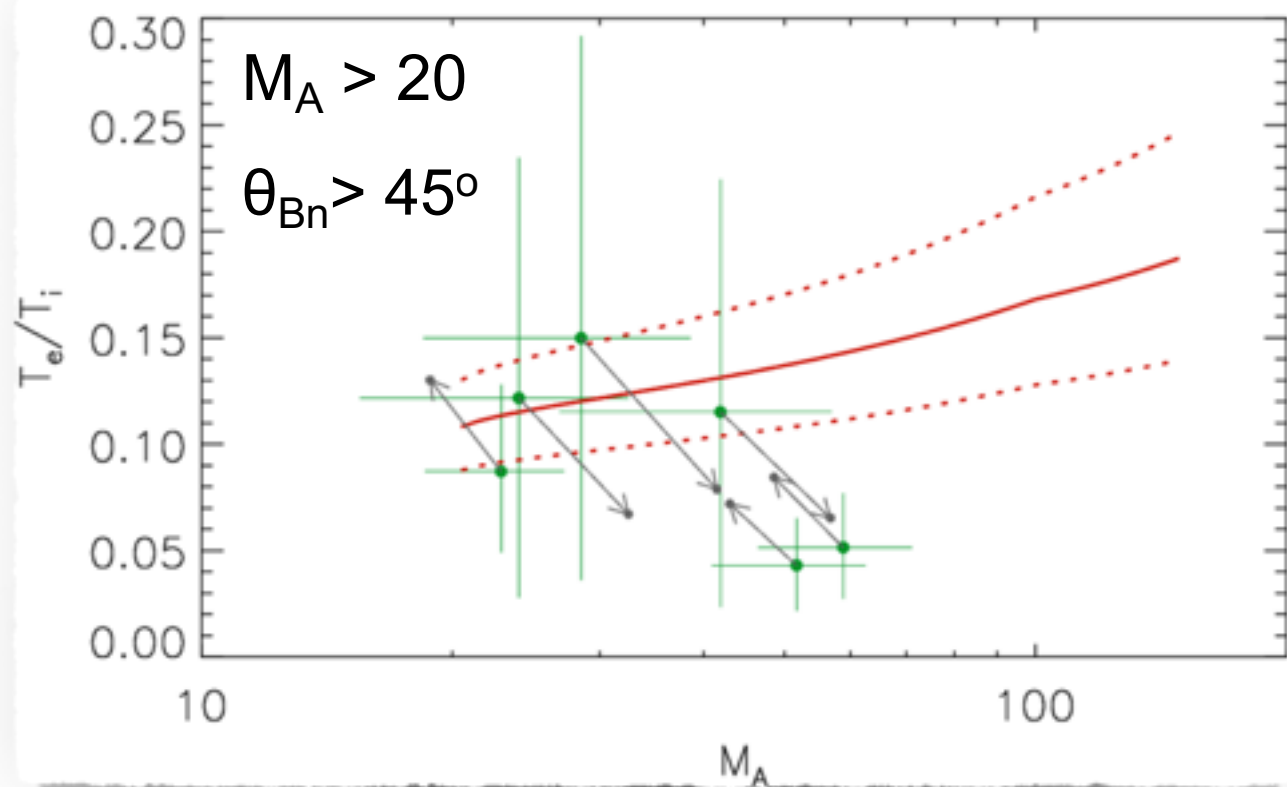
4. Stochastic Fermi acceleration (Bohdan 2017, Matsumoto 2017)

5. Adiabatic heating (compression matters)

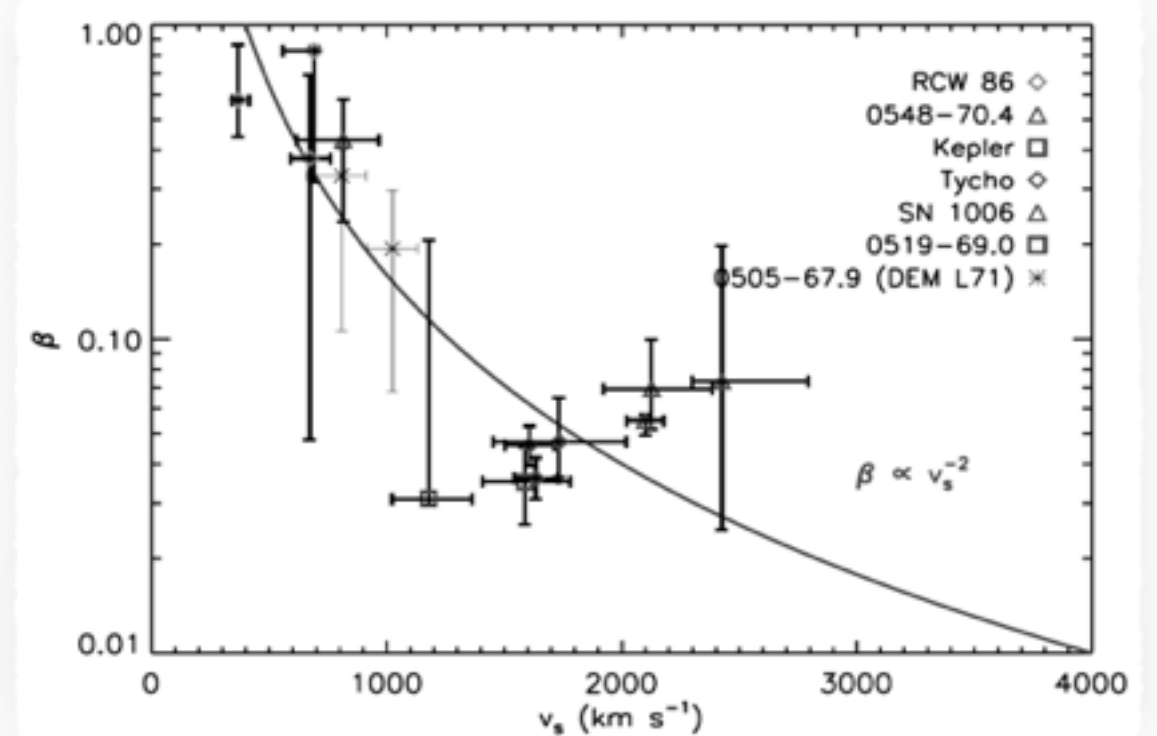


Electron heating: in-situ and observations vs. PIC

The Saturn's bow shock (Masters 2011)



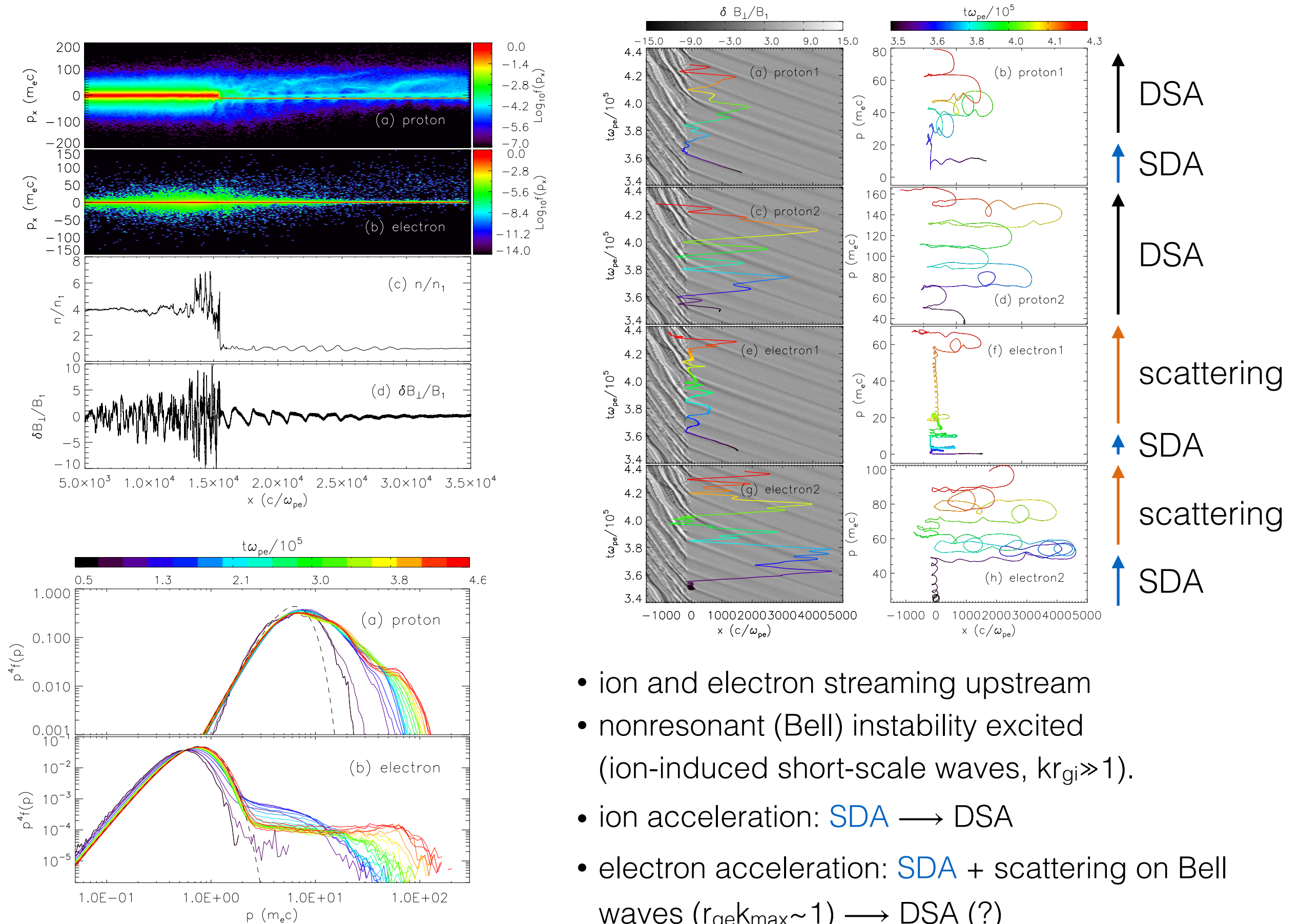
SNR shocks (van Adelsberg 2008)



$T_e/T_i \propto v_{sh}^{-2}$ is not expected

Proton acceleration

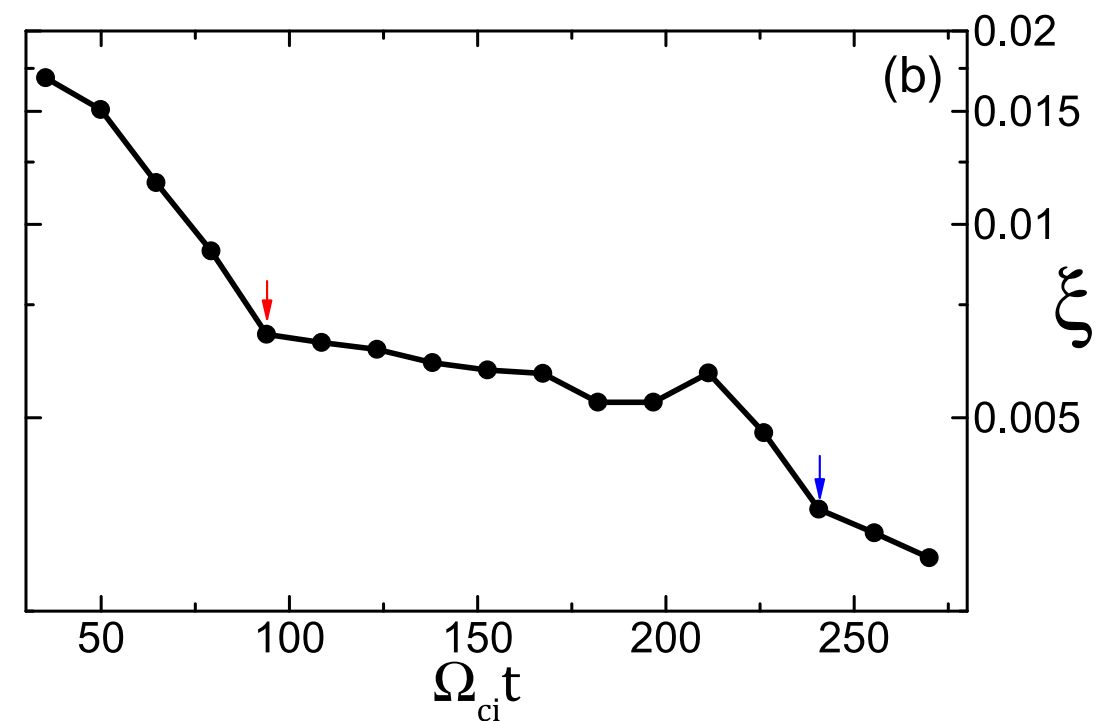
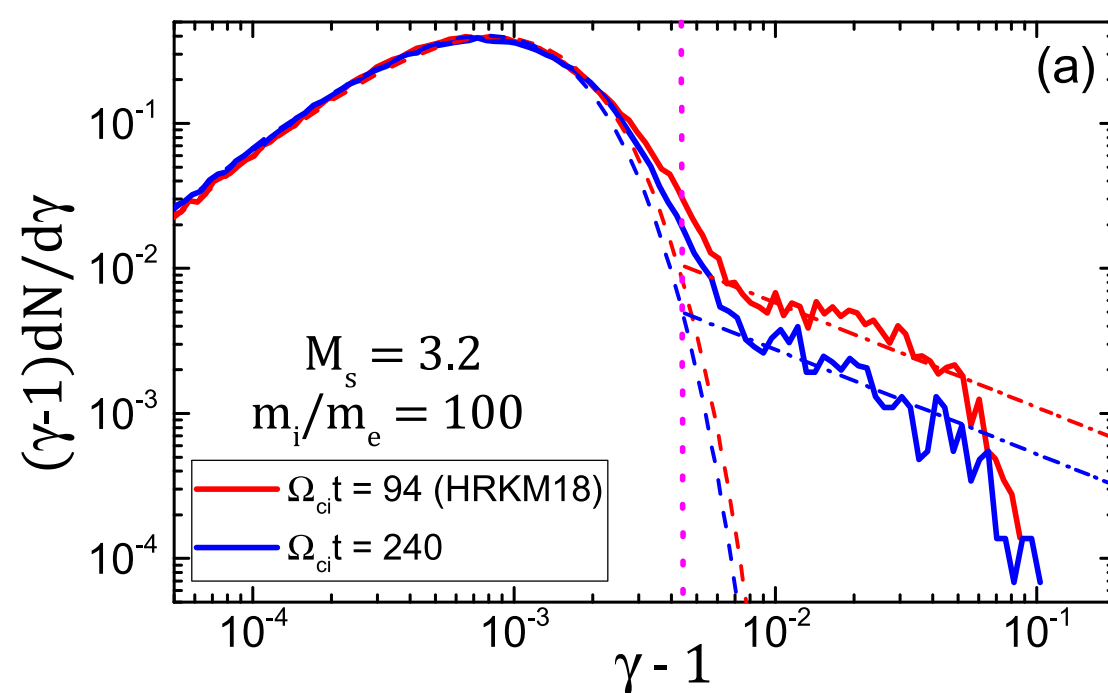
1D3V, $M_A=20$, $M_S=40$, $\vartheta=30^\circ$, $m_i/m_e=100$, $v_0=0.1c$; Park et al. 2015 Quasi-parallel shock



- ion and electron streaming upstream
- nonresonant (Bell) instability excited (ion-induced short-scale waves, $kr_{gi} \gg 1$).
- ion acceleration: SDA \rightarrow DSA
- electron acceleration: SDA + scattering on Bell waves ($r_{ge} k_{\max} \sim 1$) \rightarrow DSA (?)

Proton acceleration in low M_s high beta $Q_{||}$ shocks

- only shocks with $M_s > M_s^* \sim 2.25$ are supercritical and can accelerate protons
- proton injection proceeds like in low-beta shocks for $M_s > M_s^*$ (no electron acceleration observed)
- Proton injection fraction decreases in time

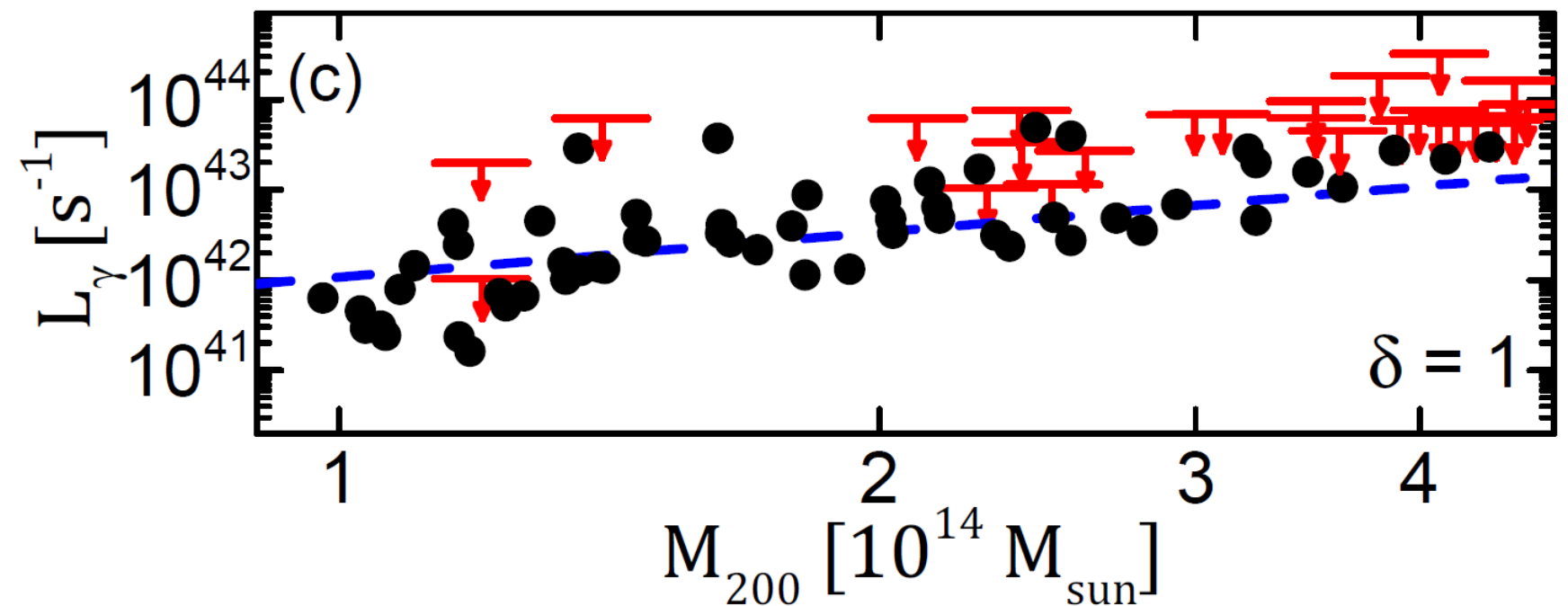


$$\xi = \frac{4\pi}{N_2} \int_{p_{min}}^{p_{max}} \langle f(p) \rangle p^2 dp$$

2D3V, $M_A \sim 18-36$, $M_s = 2-4$, $\vartheta = 13^\circ$, $m_i/m_e = 100$,
 $v_0 = 0.027c-0.067c$, $\beta = (30)-100$; Ha et al. 2019

Proton acceleration in low M_s high beta Q_{II} shocks

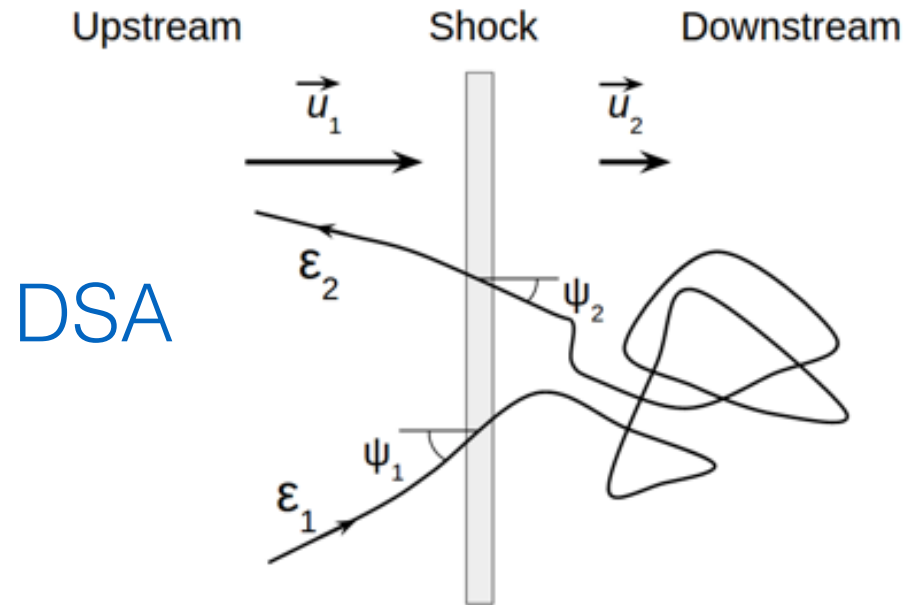
- cosmological structure formation simulations adopting [Ha et al. 2019a](#) results show that only $\sim 30\%$ of cluster shocks is Q_{II} , of which $\sim 23\%$ is supercritical
- only $\sim 7\%$ of the kinetic energy flux of entire shock population is dissipated at shocks able to accelerate protons
- average fraction of kinetic energy transferred to CR protons is $\sim 10^{-4}$
- Gamma-ray emission is thus below upper limits for clusters observed by Fermi-LAT ([Ha et al. 2020](#))



Electron injection

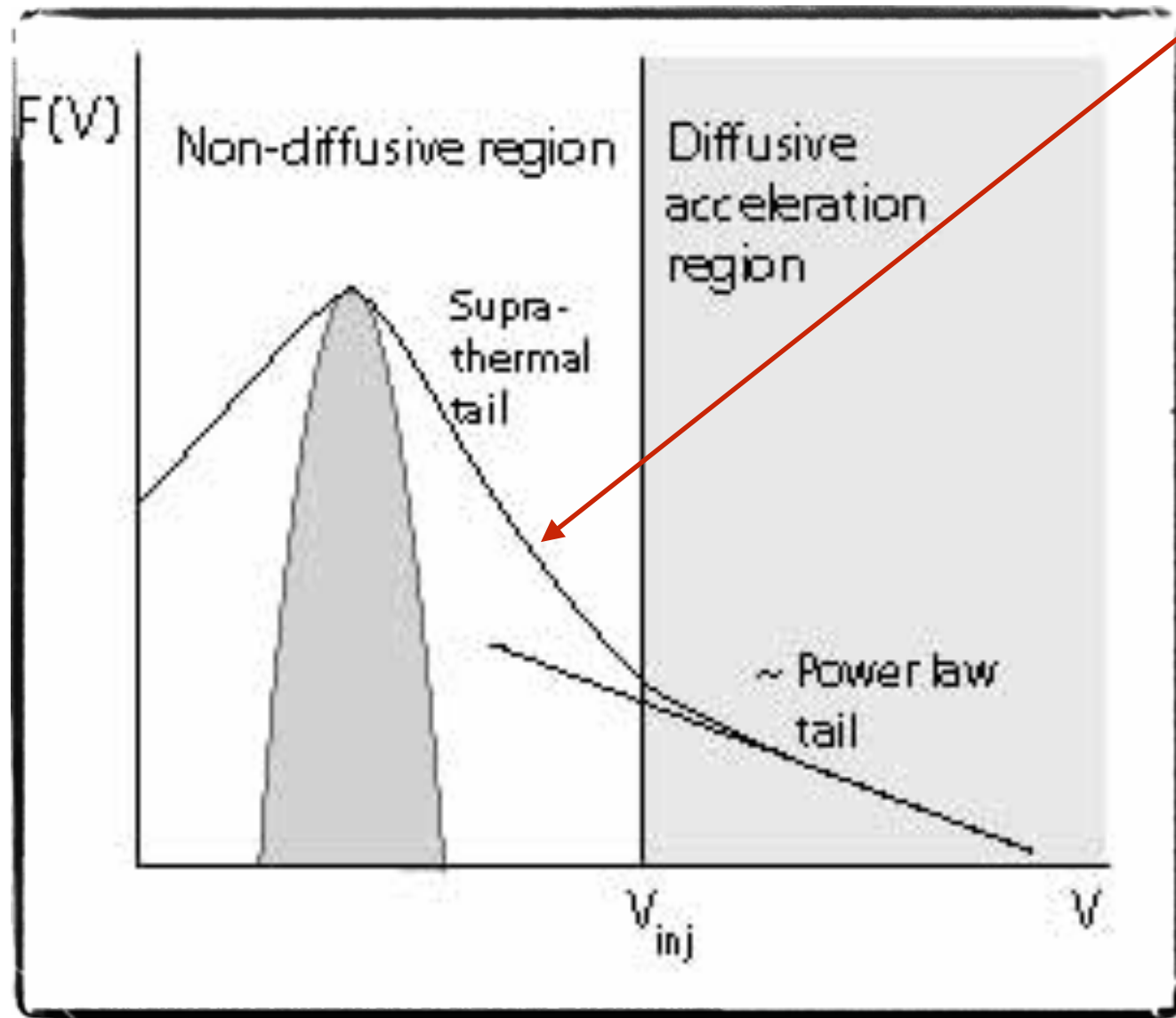
Kobzar et al., ApJ 919, 97 (2021)

Particle injection to DSA

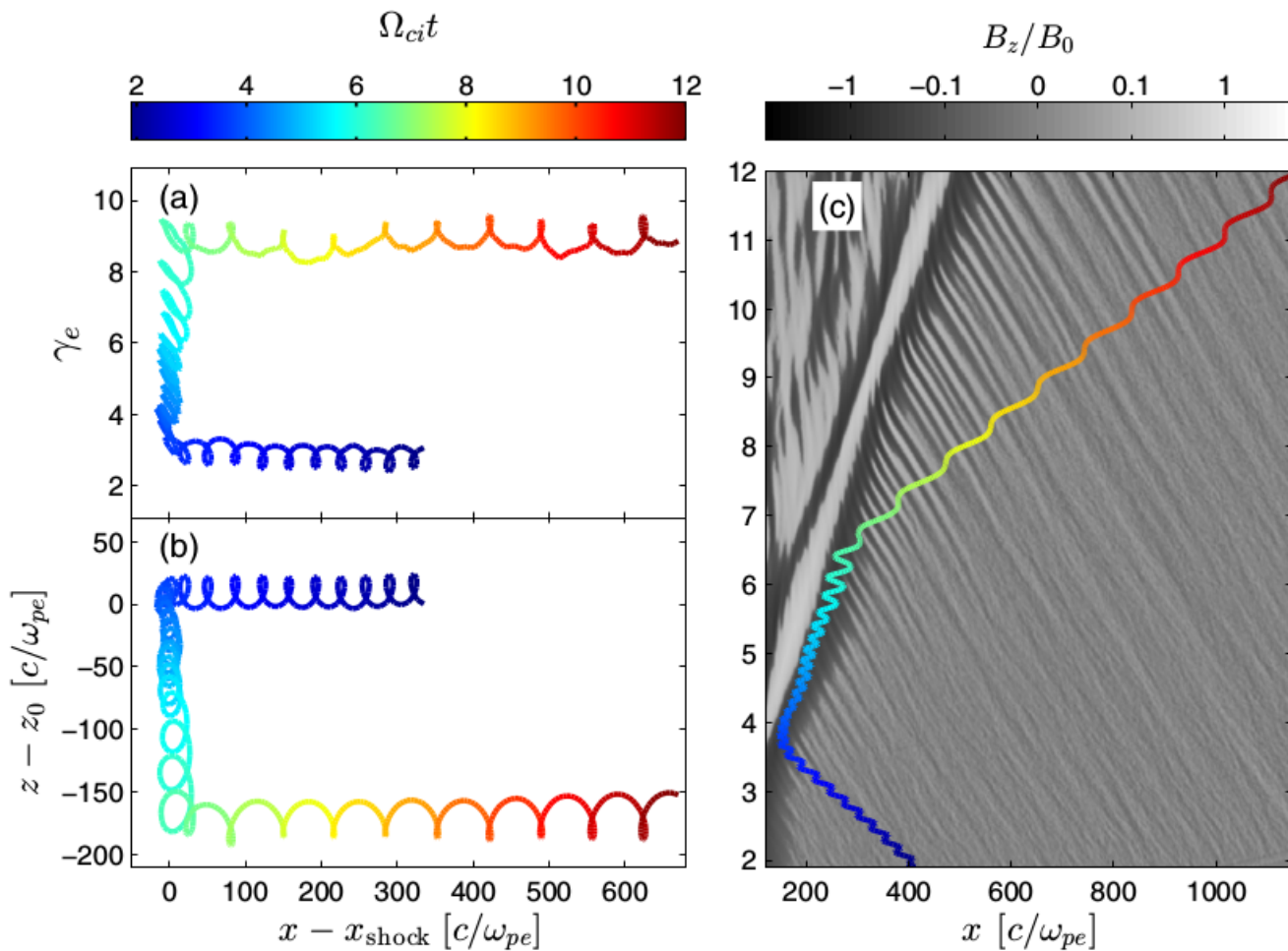


$$d_{\text{sh}} \sim (1-100) \lambda_{\text{gi}}$$

$$r_g(\epsilon_{\text{inj}}) > d_{\text{sh}}$$



Electron injection at shocks in high beta plasmas: Shock Drift Acceleration (SDA)



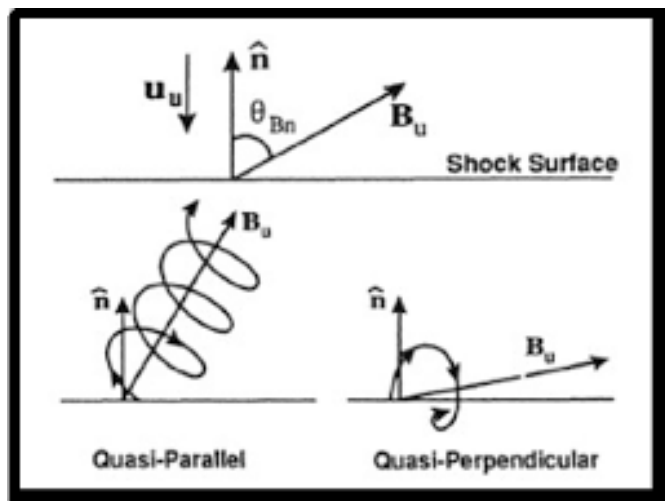
Guo et al. 2014 (2D)

- particles gain energies from the motional electric field while drifting along the shock surface due to the magnetic field gradient
- some particles can be reflected from the shock back upstream (magnetic mirror effect) and form non-thermal upstream plasma component
- works at subluminal shocks: $v_t \leq c$
- acceleration time: $\sim \Omega_i^{-1}$
- energy gain:

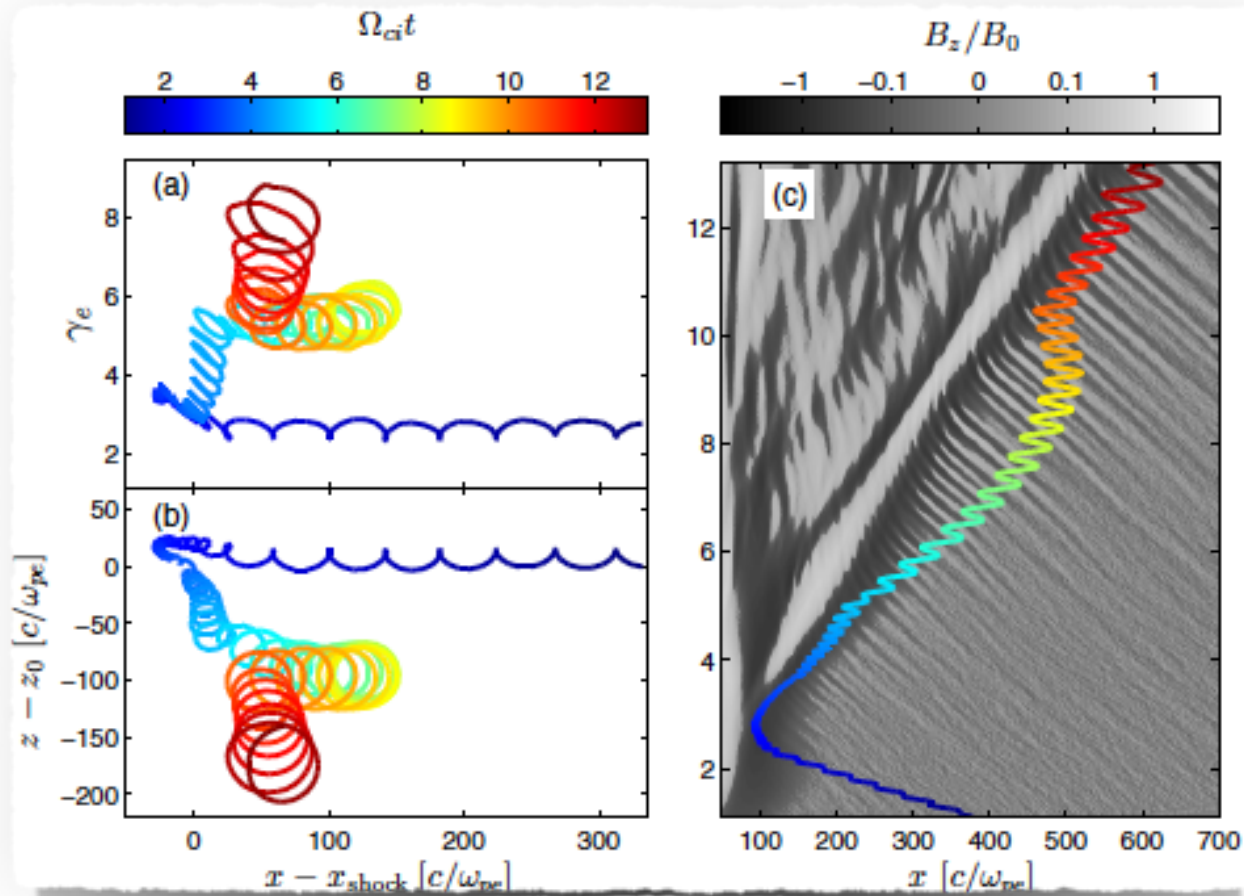
$$\Delta\gamma_{\text{SDA}} = \frac{-e}{m_e c^2} \int E_z dz$$

de Hoffman-Teller velocity:

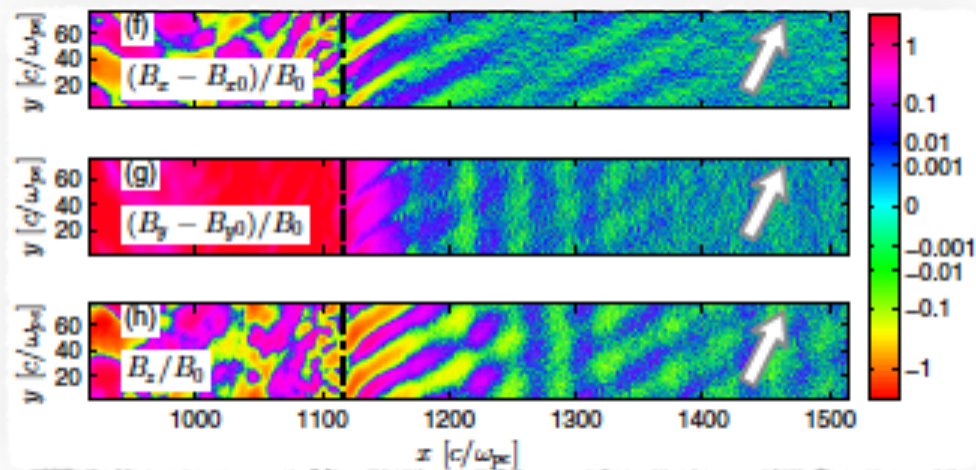
$$v_t = u_{\text{sh}}^{\text{up}} / \cos \theta_{Bn}$$



Multiple Shock Drift Acceleration cycles at quasi-perpendicular shocks

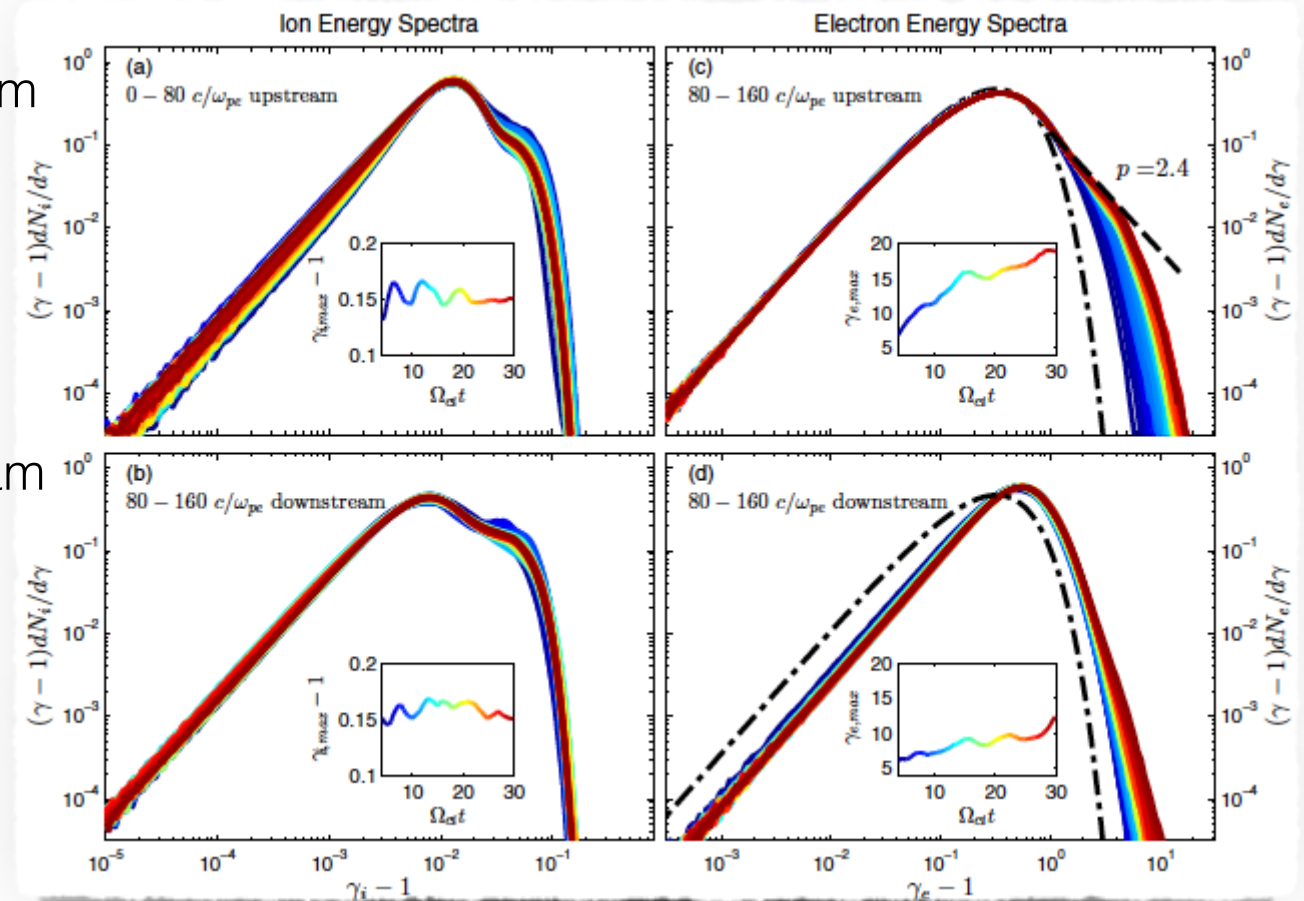


- SDA-reflected electrons scattered back towards shock by upstream self-generated waves - **DSA-like process**
- formation of **upstream** power-law spectra
- more effective at high β
- $\gamma_{\text{max}} \ll \gamma_{\text{inj}}$?



upstream

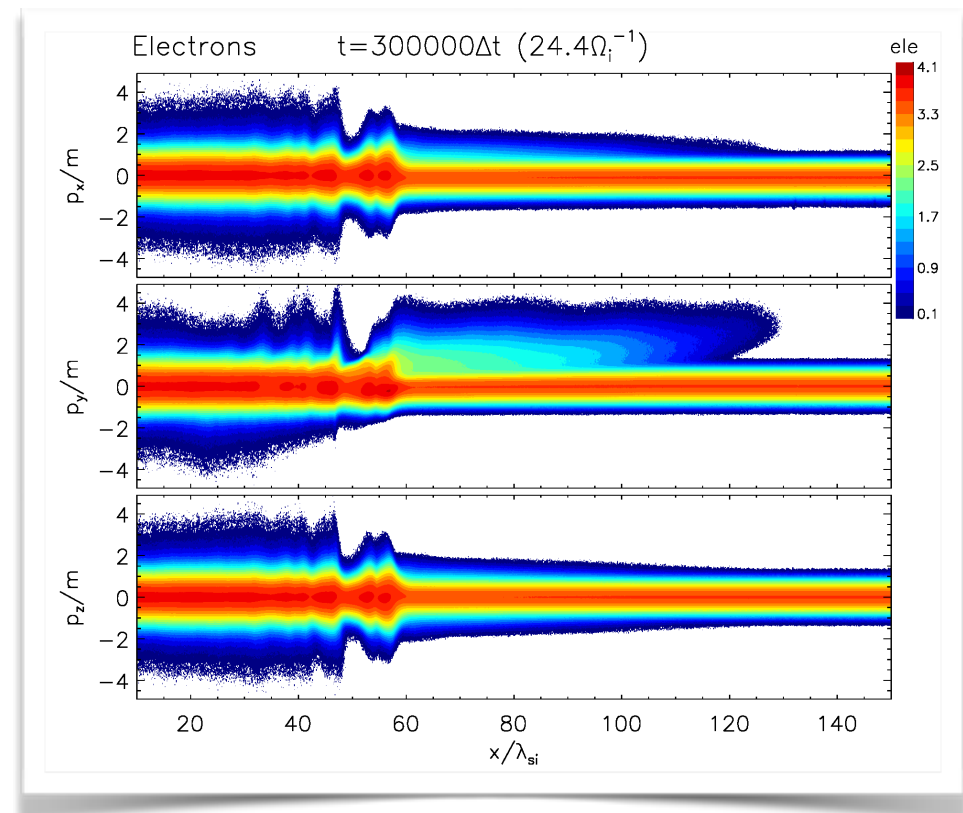
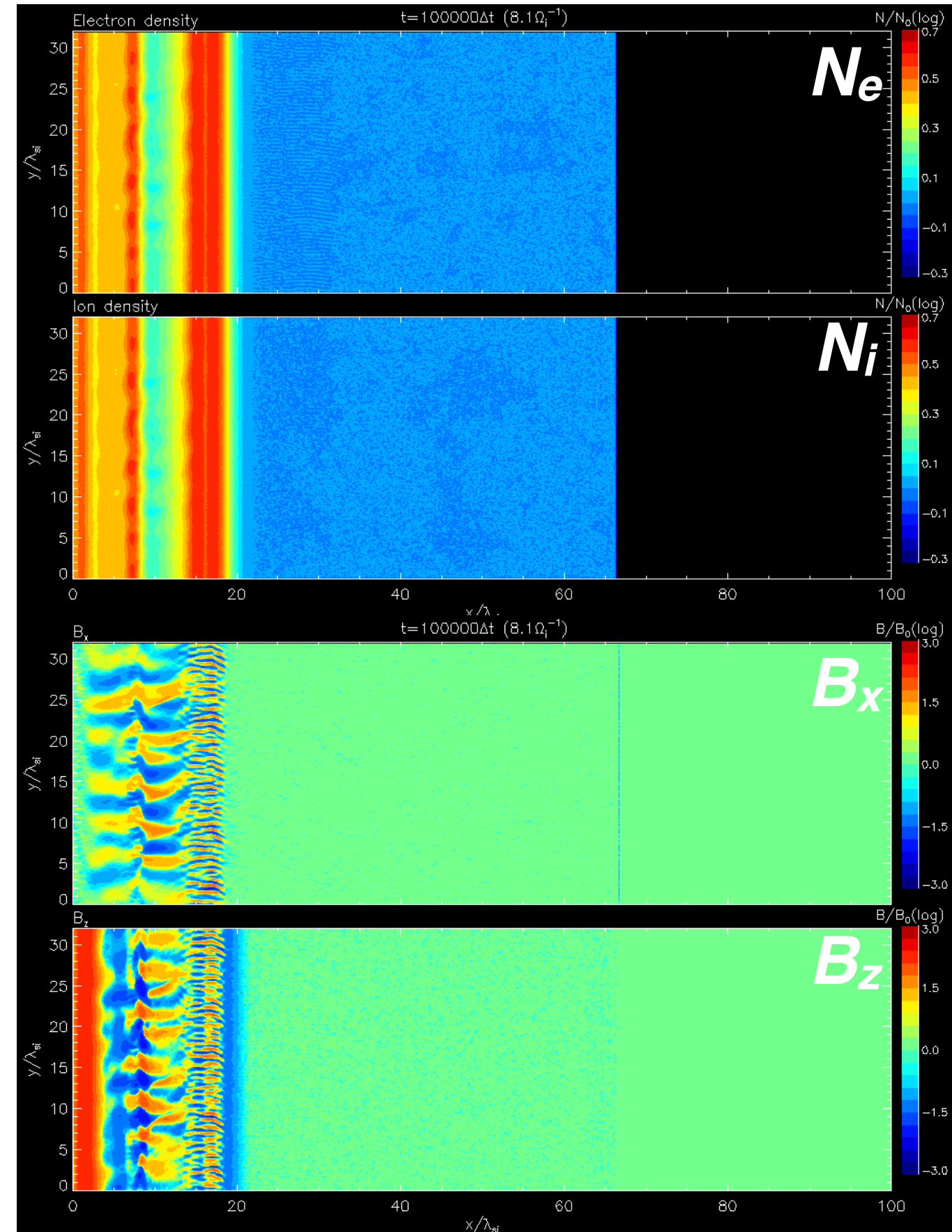
downstream



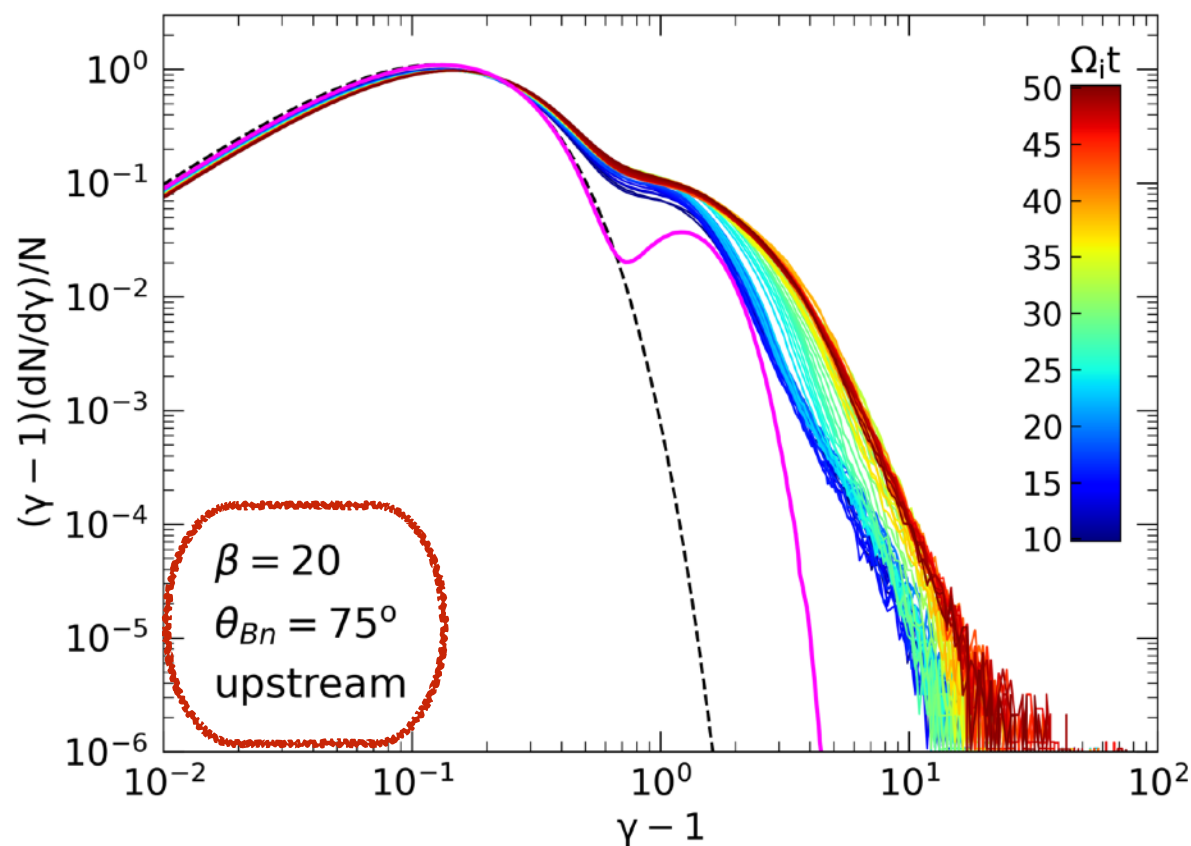
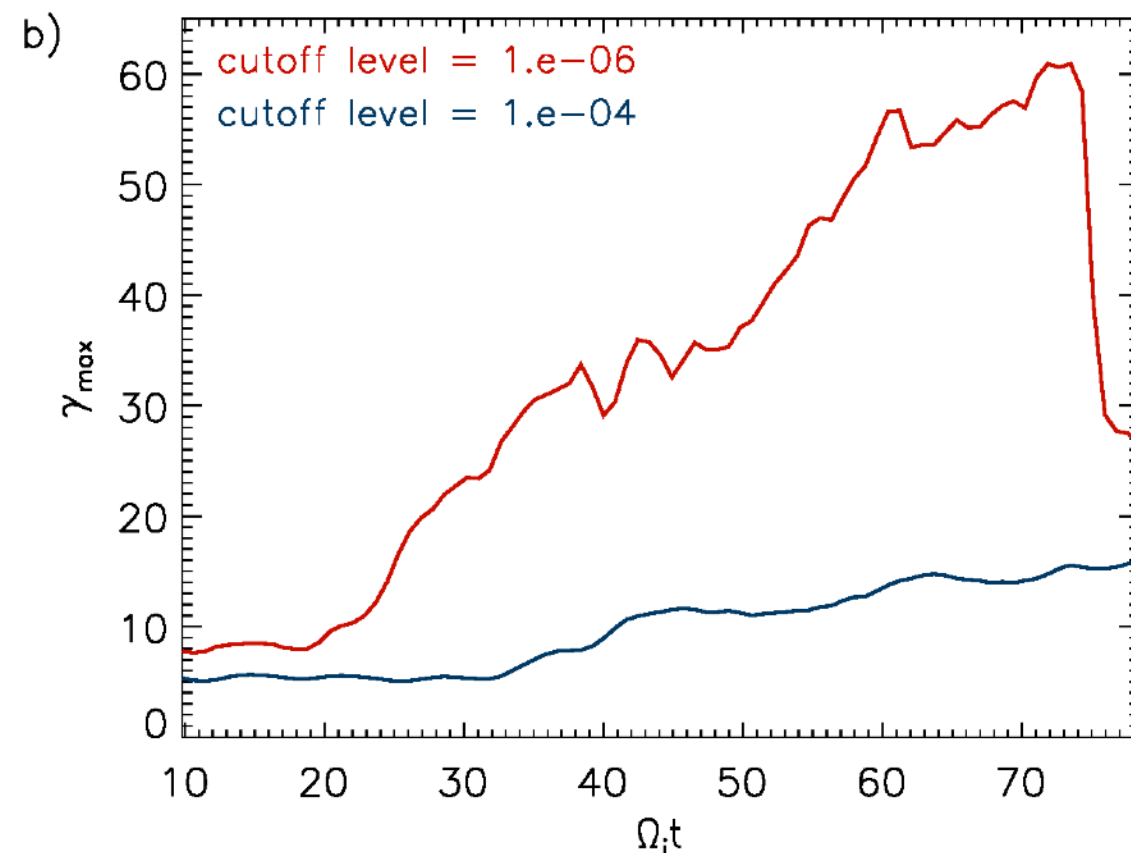
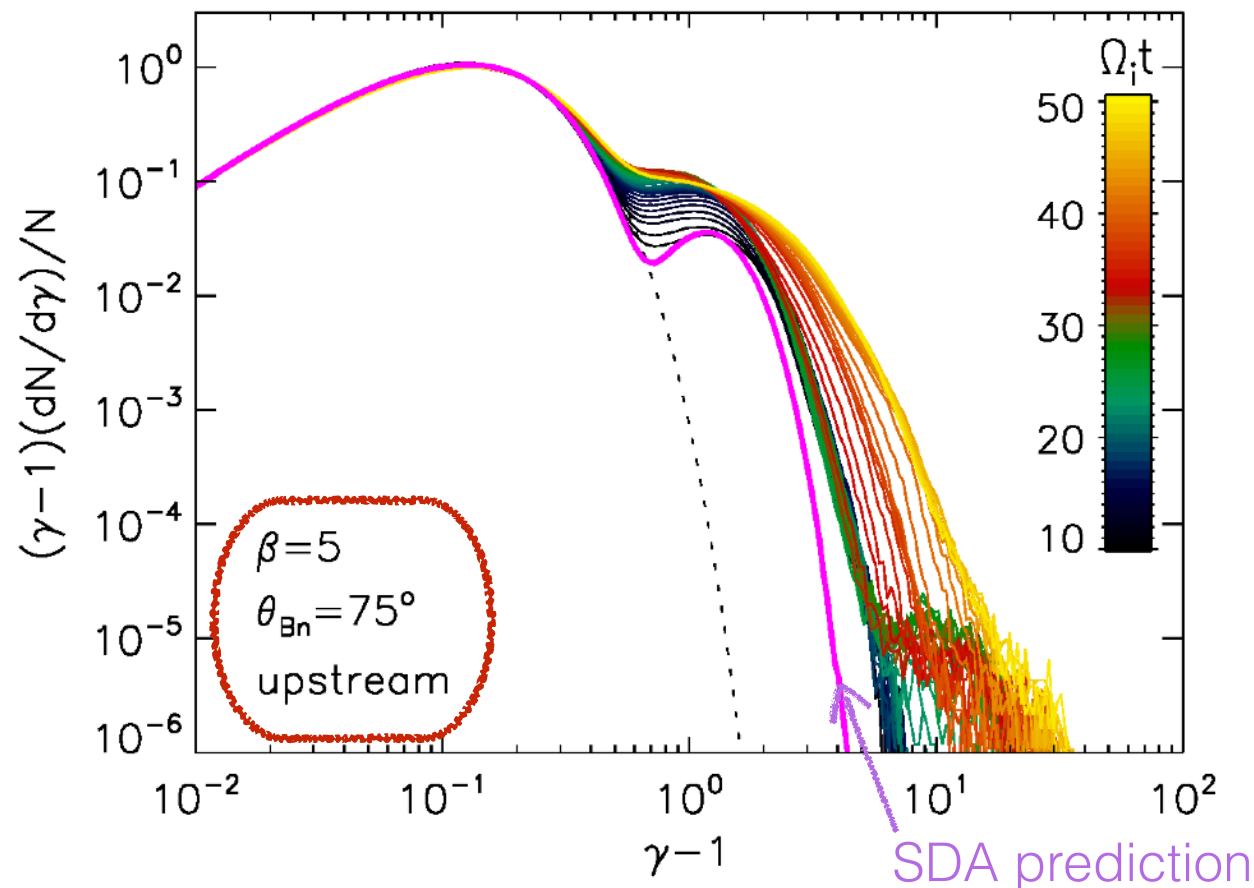
Matsukiyo et al. 2011 (1D)
 Guo et al. 2014 (2D)
 Kang et al. 2019 (2D)

Large-scale effects of the shock rippling: multi-scale turbulence

- **rippling** in the shock transition on different scales (overshoot-undershoot-2nd overshoot)
 - AIC and mirror modes
- short-scale **whistler waves** in the overshoot
- oblique and perpendicular modes of the **electron firehose instability** in the upstream, enhanced and modulated by the ripples



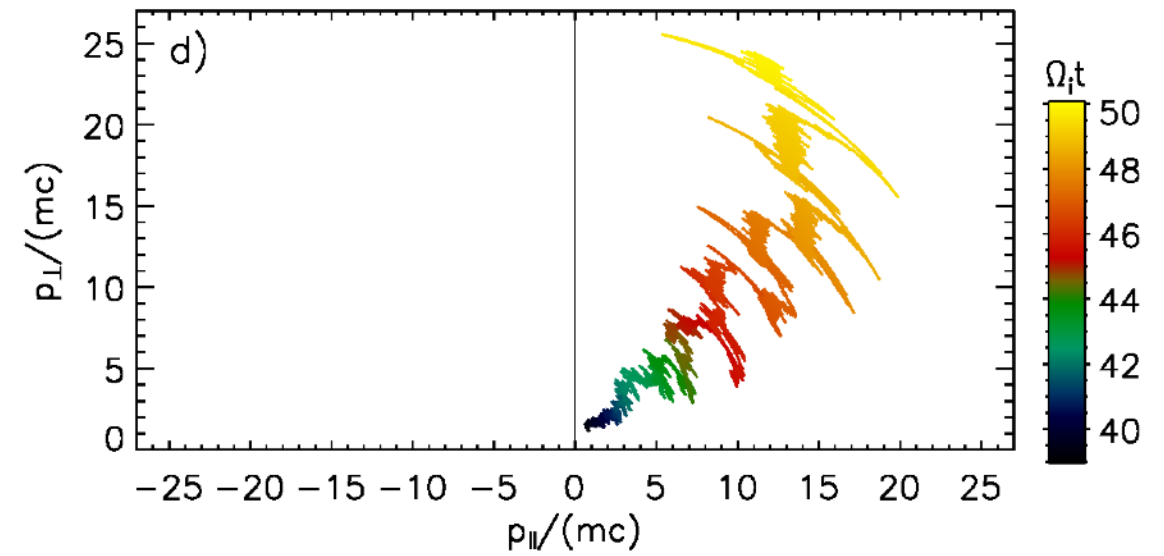
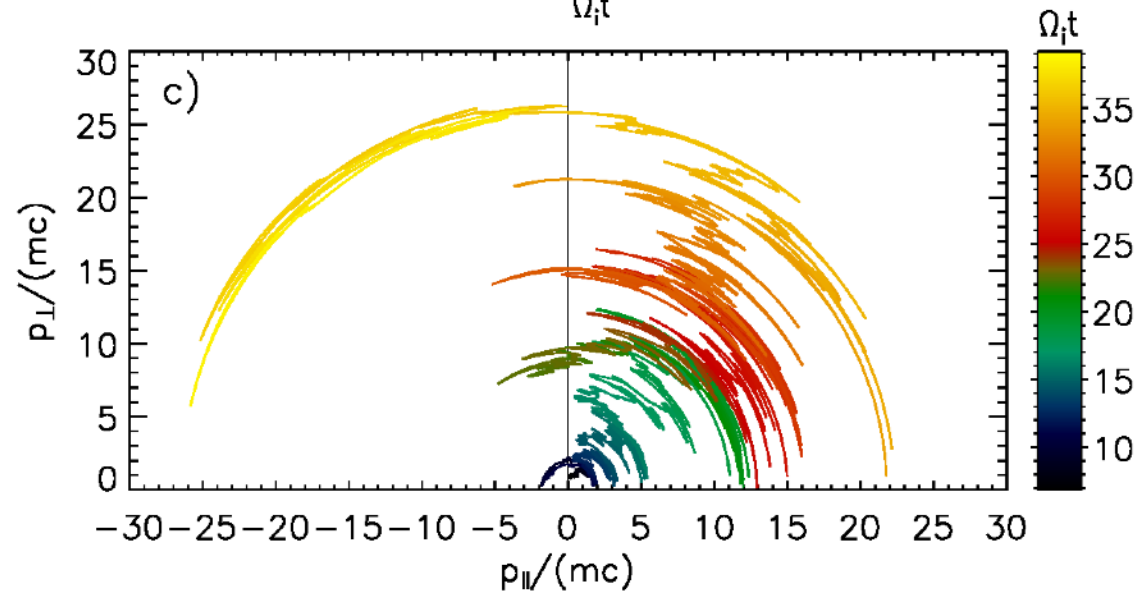
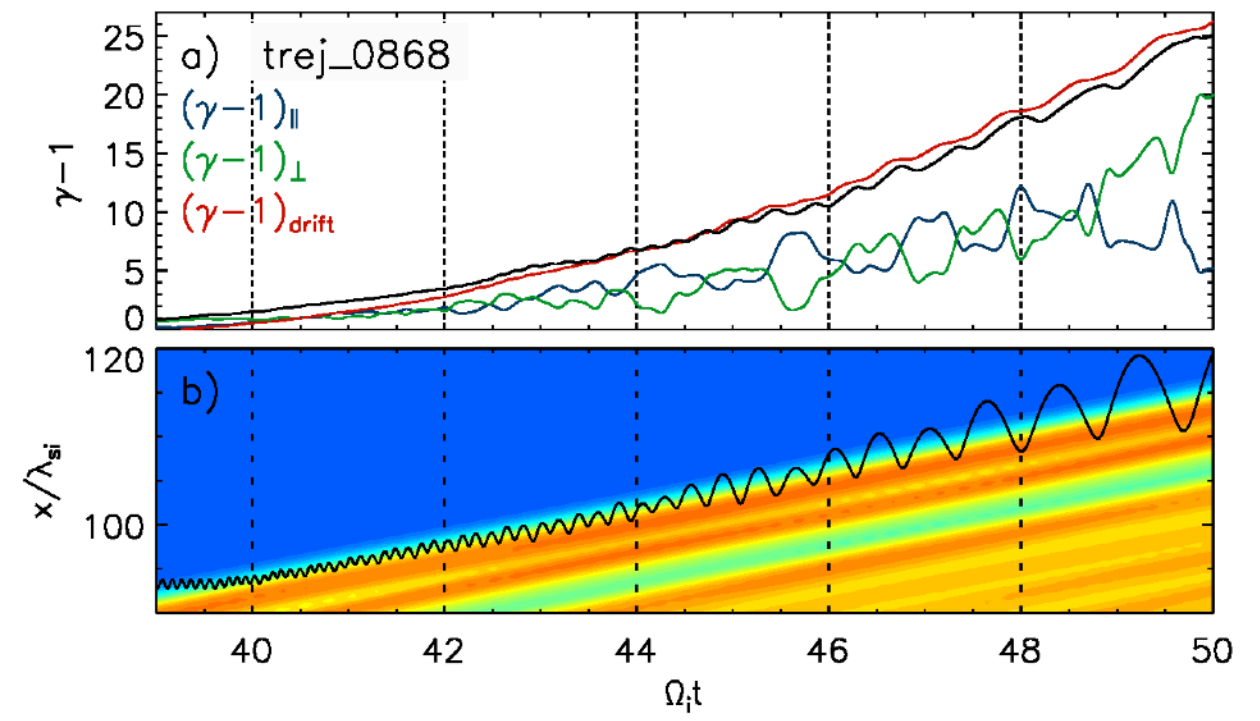
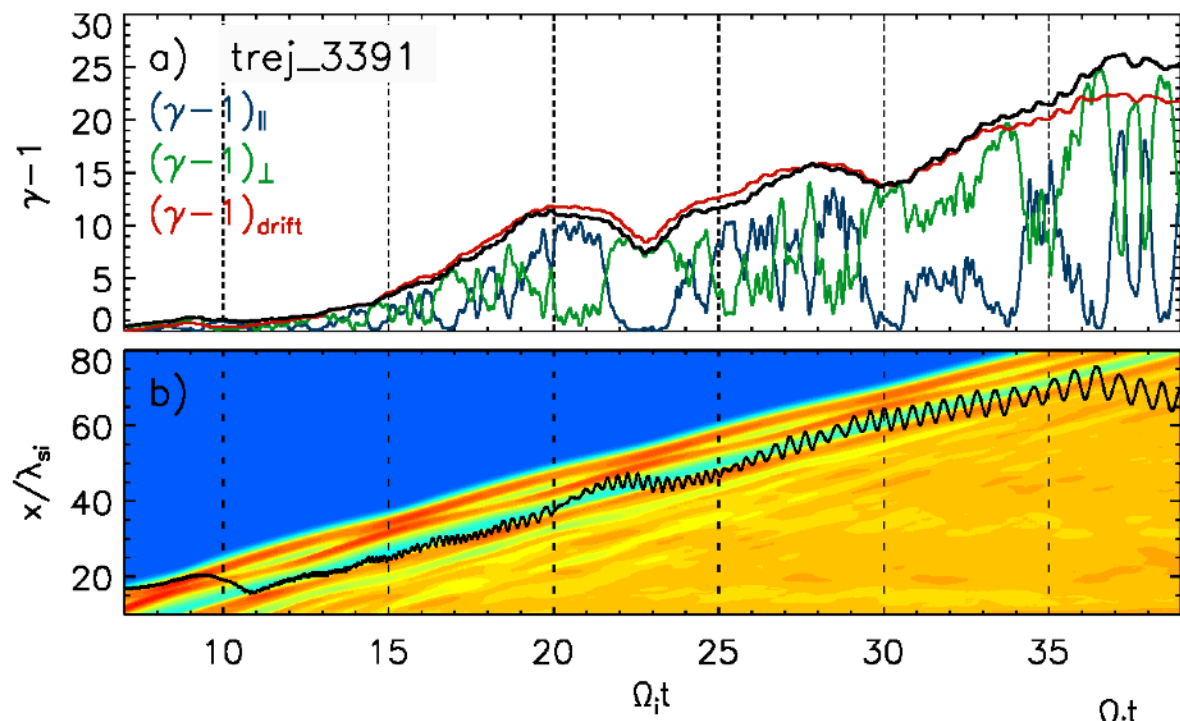
Electron spectra – time evolution



- substantial increase in non-thermal tail production efficiency coincident with the onset of the shock rippling at $\Omega_{ci}t \approx 25$
- maximum electron energy sufficient for injection to DSA: $\gamma_{inj} \approx 25$ ($p_{inj} \sim 3p_{th,i}$)

$$\gamma_{max,up} \approx 40 - 60$$

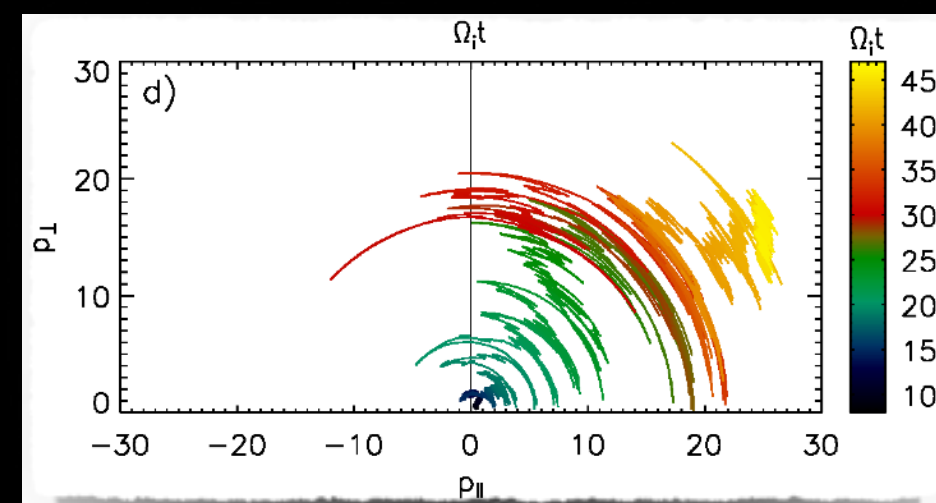
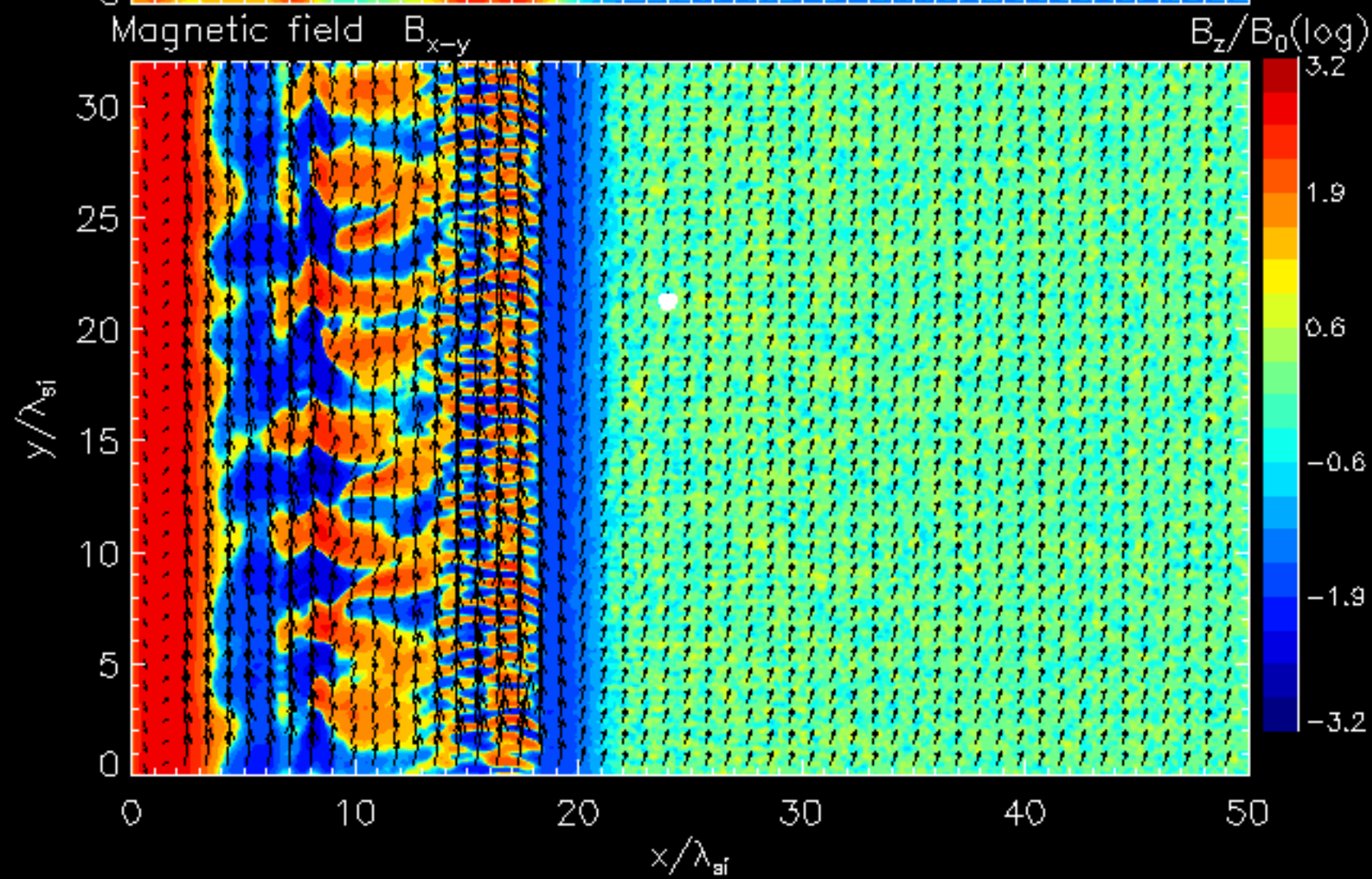
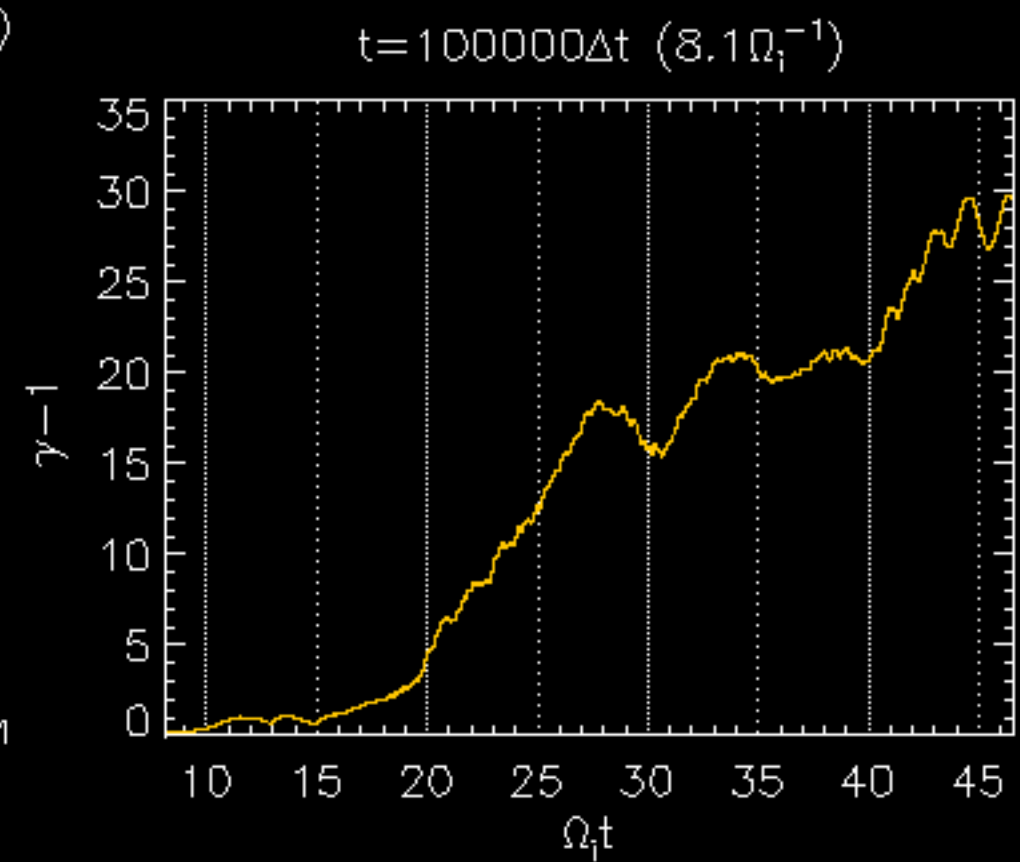
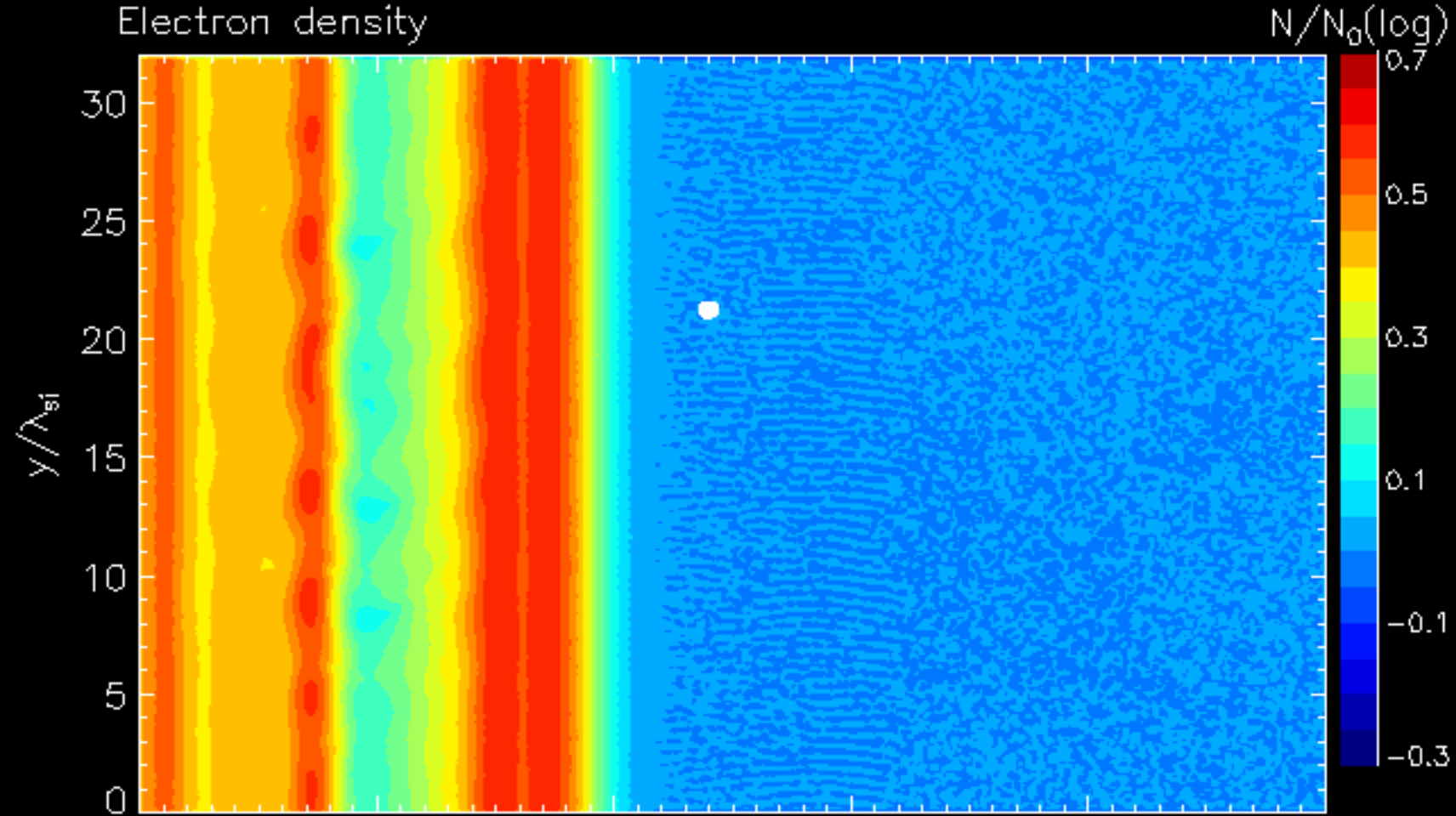
- upstream spectra weakly depend on beta



- most accelerations associated with an increase in p_\perp
- strong **pitch-angle scattering** (arcs in p_\parallel - p_\perp momentum space)
- energy gain mostly through the drift along motional electric field:

$$\Delta\gamma_{\text{drift}} = (-e/m_e c^2) \int E_z dz$$

→ Stochastic Shock-Drift Acceleration (SSDA; Katou & Amano, 2019)



Summary

- kinetic modeling of particle acceleration at collisionless shocks requires multi-dimensional and large-scale effects to be taken into account
- in high Mach number shocks the Weibel instability amplifies magnetic field; PIC results combined with in-situ data allow extrapolation towards SNR shock conditions
- PIC modeling also allows us to derive a model for the electron-ion temperature ratio in agreement with in-situ data
- 1D studies of proton injection suggest proton acceleration efficiency at ICM shocks much lower than in low- β plasmas - detection of gamma-ray emission requires sensitive observations (LHAASO, CTA)
- protons injected only in supercritical quasi-parallel shocks with $M_s > 2.25$
- electron injection at low Mach number shocks occurs at quasi-perpendicular sub-luminal shocks
- electron injection proceeds mainly through the stochastic SDA process in multi-scale turbulence in the shock transition